UNIVERSITAT POLITÈCNICA DE VALÈNCIA

ESCUELA TÉCNICA SUPERIOR DE INGENIEROS DE CAMINOS, CANALES Y PUERTOS

Análisis estructural del Puente Colgante de Clifton situado en Bristol, Reino Unido.

Tomo 1 – Memoria

Trabajo final de grado

Titulación: Grado en Ingeniería Civil

Curso: 2015/16

Autor: Toms, Cameron Ian

Tutor: Payá Zaforteza, Ignacio Javier

Cotutor: —

Valencia, junio de 2016

Contents

Abstract

This project is an evaluation and analysis of the principal elements of the Clifton Suspension Bridge in Bristol, UK. The analysis is done with a numerical method solved on a computer and a graphical method called graphic statics. The methods and the designs for the bridge are studied in their historical context. Despite the fact that graphic statics is more limited than the numerical method, it produces results that agree with the numerical analysis and physical tests. The errors caused by graphic statics are analysed and discussed. The results show that the bridge was well designed for the original design loads, and that the current restrictions on vehicles well suited. Finally the bridge and several alternative designs are qualitatively evaluated in terms of the quality of design and their value in a social and historical context.

Resumen:

Este proyecto es una evaluación y análisis de los elementos principales del puente colgante de Clifton en Bristol, Reino Unido. El análisis se hace por un método numérico en ordenador y un método gráfico que se llama estática gráfica. Los métodos y los diseños para el puente se investigan en su contexto histórico. A pesar del hecho de que la estática gráfica tiene más limitaciones que el método numérico, produce resultados que están de acuerdo con el análisis numérico y los ensayos físicos. Los errores causados por la estática gráfica se analizan y se discuten. Los resultados muestran que el puente fue bien diseñado para las cargas de diseño originales, y que las restricciones actuales están bien. Al final, el puente y varios diseños alternativos se evalúan cualitativamente desde el punto de vista de la calidad de diseño y su valor en un contexto social y histórico.

Resum:

Este projecte és una avaluació i anàlisi dels elements principals del pont penjoll de Clifton en Bristol, Regne Unit. L'anàlisi es fa per un mètode numèric en ordinador i un mètode gràfic que s'anomena estàtica gràfica. Els mètodes i els dissenys per al pont s'investiguen en el seu context històric. A pesar del fet de que l'estàtica gràfica té més limitacions que el mètode numèric, produïx resultats que estan d'acord amb l'anàlisi numèrica i els assajos físics. Els errors causats per l'estàtica gràfica s'analitzen i es discutixen. Els resultats mostren que el pont va ser ben dissenyat per a les càrregues de disseny originals, i que les restriccions actuals estan bé. Al final, el pont i diversos dissenys alternatius s'avaluen qualitativament des del punt de vista de la qualitat de disseny i el seu valor en un context social i històric.

1. Introduction

Modern civil engineering almost exclusively uses numerical methods of analysis in the design of buildings and civil structures. Civil engineering students are taught how to do structural analysis with hand calculations while computers analyse complex models by solving thousands of matrices. However the mathematics behind these methods is a relatively new invention. Many of the world's most famous monuments, palaces and bridges were designed and constructed before the invention of these numerical methods. The primary aim of this project is to compare an alternative method of analysis with a modern numerical method, and explore more deeply the history of structural analysis and its effect on construction.

To compare the methods, they will be used to analyse the Clifton Suspension Bridge in Bristol, UK. The bridge itself is one of the oldest surviving examples of early suspension bridge design and is an illustration of how the evolution of technology and the understanding of structures affects the way structures are designed. The results of the analysis will also be used to evaluate the design of the bridge, which was built in a time when the behaviour of suspension bridges was poorly understood.

Unlike the sciences, where the aim is investigation and the emphasis is on what is not understood, the emphasis in structural engineering is on what we already know. It often seems that things that we do not understand or cannot calculate are avoided in favour of something that we understand. The history of suspension bridges is one full of experimentation, mistakes, unknowns and guesses. It is this side of engineering that intrigues me.

2. Objectives

The objectives of this work are to analyse part of the structure of the Clifton Suspension Bridge in a simplified manner using a graphical and numerical method of structural analysis. The results of the analysis will permit an evaluation of the design of the suspension bridge and a comparison of the two analytical methods.

3. Methodology

The project will be put into historical context so that the thinking behind the design of the Clifton Suspension Bridge can be better explained. The analysis of the bridge will be broken down into parts primarily encompassing the transversal deck girders, the suspension chains, and the longitudinal girders. This will provide enough information to make a critical evaluation of the superstructure of the bridge. The analysis will be carried out using both the graphical and numerical methods where possible and will be based on the design load used during construction and the loads that the bridge is subjected to today. The results of the two methods will be compared in order to identify the causes of any errors and permit a quantitative and qualitative evaluation of the methods.

4. Historical Context

4.1. A history of suspension bridges

Suspended bridges made of ropes, bamboo and iron chains have existed for millennia (Body, 1976), however the first modern suspension bridges came with the advent of the use of structural iron. The Coalbrookdale Bridge in Shropshire, UK, was built in 1779 and is credited as being the first cast iron bridge. Although the use of the material was novel, the structure was not: the bridge uses the same circular arch design that the Romans had been using 2000 years earlier. This trend of building iron bridges with structures more suited to being made of wood or stone continued for decades; in 1802 the French government ordered three new 'modern' bridges to be built – all had structures based on wooden and stone bridges (Grattesat, 1978).

The first step was the invention of the iron eyebar, patented by Samuel Brown in England, 1817. Three years later he built the Union Chain Bridge over the River Tweed. With a span of 137m, it was the longest suspension bridge in the world at the time (Grattesat, 1978). It was exceeded by Thomas Telford's bridge over the Menai Strait in 1826, whose largest span is 177m. The Menai Suspension Bridge is regarded by many as the first important step in the history of suspension bridge design (Gimsing, 1984).

At the same time in France, iron suspension bridges were being constructed. The Tournon Bridge over the Rhône, built in 1825 by Marc Seguin, used innovative cables made of 3mm iron threads to support the deck (Gimsing, 1984). Although this method became popular in France, it was not widely adopted elsewhere because of the difficulty of construction and poor quality control (Drewry, 1832).

Figure 1. The Brooklyn Bridge, with vertical hangers and inclined stays visible (User:Postdlf, 2005).

As technology became more refined, the size of the bridges increased. In 1849, Charles Ellet Jr. built the Wheeling Bridge over the Ohio River in the USA. With a span of 308m, it was significantly larger than anything built before it and was supported with iron cables. Five years later it collapsed during a storm. Following this and the collapse of several other bridges in high winds, an emphasis was placed on the safety and stiffness of bridges. Ferdinand Arnodin improved deck design by using the parapet to improve stiffness and Seguin invented cable-winding machines to so that cables could be constructed on-site (Grattesat, 1978).

The Brooklyn Bridge, New York (see fig. 1), was completed in 1883 by John Roebling and is a good illustration of the progression of suspension bridge design in that period. The only mathematical theories to describe the mechanics of suspension bridges at that time were *1st order theories* such as Rankine's, published in 1869 (Buonopane and Billington, 1993), which describe the bridge according to its undeflected shape. This meant it was not possible to calculate how the loads in the structure changed as it deflected under load. To make up for this, the Brooklyn Bridge is supported by a combination of cable-stays as well as suspended cables and has a deep 'stiffness truss'. The entire structure is highly indeterminate and heavily over-engineered; Roebling said that if all the suspended cables where removed, the bridge would still not collapse (Gimsing, 1984).

Shortly afterwards in 1888, Joseph Melan published his 2nd order *deflection theory* (Gimsing, 1984). Although it was difficult to implement by hand, it took into account the displacements of the suspension cables under load, so the results were more accurate than using the 1st order geometry. Gimsing believes that this marked the beginning of a move towards mathematically simpler designs, such as the Williamsburg Bridge, built in 1903. It has a similar span to that of the Brooklyn Bridge (490m) but no stays, as their effect was impossible to calculate. Unlike earlier designs, bridges from this period have cables the attach to the bottom of the stiffness truss, as it is more economical. The *lateral force theory* developed by Moissiff and Hudson in 1932 meant that the effects of horizontal wind loads could be calculated, making the 'wind girder' in the decks of older bridges unnecessary (Gimsing, 1984). These advances in mathematical ability, writes Gimsing in *Cable Supported Bridges* (1984), meant that engineers became increasingly reliant on calculations and were 'blindly trusting of results'. Although the behaviour of the bridge could still not be completely calculated, there started a trend towards extreme slenderness. Bridge decks were built with ever more slender and flexible decks because they were calculated to be adequate. A good example is the Golden Gate Bridge, San Francisco (see fig. 2), which had a span to depth ratio of 168 when built. The problem of torsional stiffness and dynamic air pressures came to light after the spectacular collapse of the Tacoma Narrows bridge in light winds. The Golden Gate Bridge was subsequently modified and investigation was made into the effects of aerodynamics (Gimsing, 1984). New analytical methods were developed.

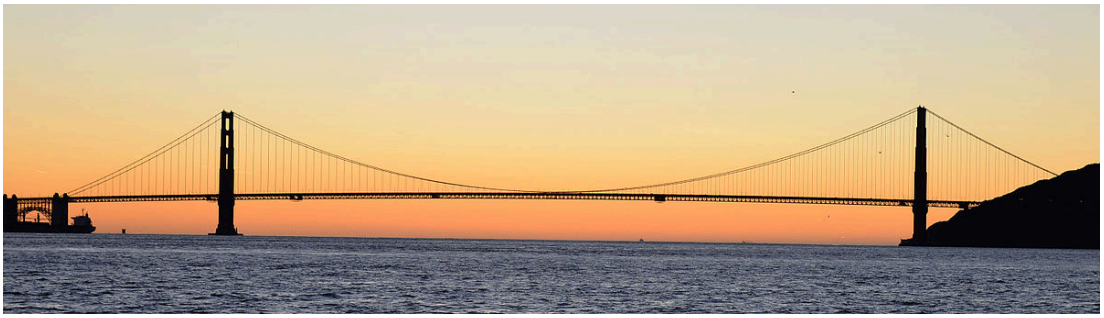

Figure 2. The Golden Gate Bridge, San Francisco (WPPilot, 2015).

Figure 3. Photograph of the Severn Bridge, showing inclined hangers and aerodynamic deck profile (Edwards, 2007).

After the Second World War there was an increase in building activity and designs began to tend in the opposite direction to those of the 1930s. Gimsing (1984) notes that the Mackinac bridge in Michigan, US, is designed for a maximum wind speed of 995km/h – far in excess of what is required.

Further advances in structural analysis lead to the construction of the first cable-stayed bridge in 1956. It has become the preferred form of long-span bridge as it allows for a cantilever method of erection.

In 1959, the Tancarville Bridge, France, became the first suspension bridge outside of America to have a span of more than 500m. Unlike American-style bridges, which had steel towers, the Tancarville Bridge had concrete towers and a continuous deck that ran through the centre of the towers. A culmination of modern analytical and construction techniques permitted the building of the Severn Road Bridge, UK in 1966 (see fig. 3). Its very slender deck (with a span:depth ratio of 324) that had been unthinkable just twenty years earlier was made possible by an aerodynamic box girder deck section which gave high torsional stiffness and cost savings over traditional methods. An intersecting arrangement of inclined hangers provided sufficient vertical damping (Gimsing, 1984).

Suspension bridges continue to be used in the largest spans today, as they can be made more cheaply and with less material than other bridges. The longest suspended span to date is the Akashi-Kaikyo Bridge, in Japan and measures almost 2000m (Miyata et al., 2002).

4.2. Graphical methods of structural analysis

Although Newton published his theories on mechanical mathematics in 1687, the use of mathematics in structural engineering and design is still relatively modern. Computers have only been used in structural design and analysis for the last half a century, yet it is now unthinkable the it could exist without them. One of the earliest records of structural analysis is Giovanni Poleni's *Memorie istoriche della gran cupola del tempio Vaticano*, published in 1748. In it, Poleni examines the cupola of St. Peter's Basilica in the Vatican and formulates a plan to have it repaired.

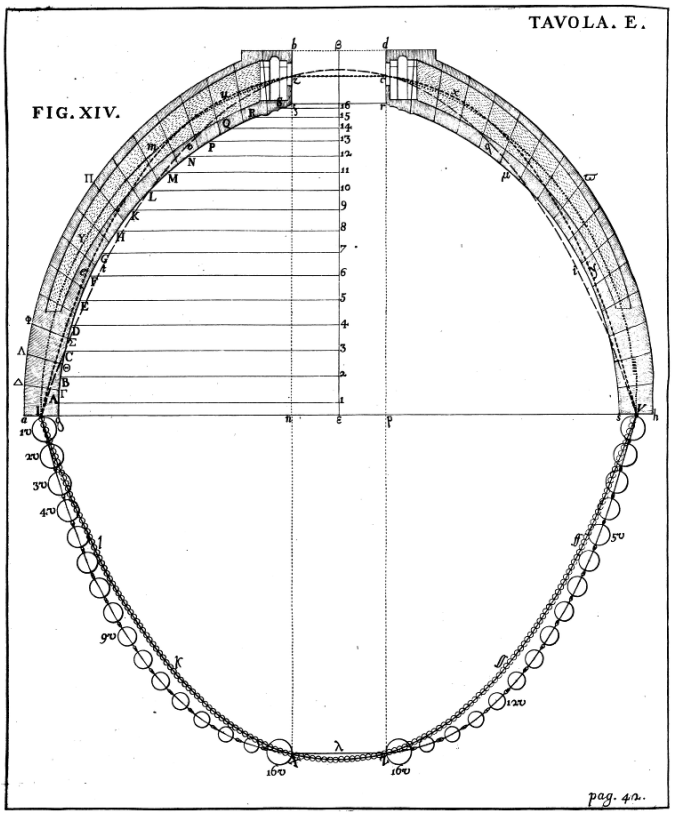

Figure 4. Poleni's diagram of the cupola (Poleni, 1748). Compressive loads in the dome above are compared to the tensile loads that occur in a catenary.

The first theories regarding suspension bridge design were published by Claude Navier in 1823, having studied early suspension bridges in England. However it only provided basic calculations about the effect of wind loading, with Navier noting that 'the accidents that would result from this action can be appreciated and prevented only from knowledge provided by observation and experience,' (Buonopane and Billington, 1993). The changes to the design of bridges over the last 200 years illustrate how much our understanding has advanced since then. However, as the use of computers for calculation only became commonplace in the 1950s, many famous landmarks – such as the Brooklyn Bridge – were built without this analytical power.

Graphical methods of analysis are an alternative to modern numerical methods. The architect Antoni Gaudí famously built models of strings and weights (see fig. 5), which, when viewed upside down, represented the force paths in a building. The graphical method addressed in this project is called graphic statics, which can be done using simple drafting tools. It has its origins in the works of the Dutchman Simon Stevin and was further developed by James Maxwell and Luigi Cremona in the nineteenth century (Baker et al., 2013). The graphic statics method introduced by Cremona for solving trusses became so popular that is often called the Cremona method.

Figure 5. Gaudí's force model of the Colònia Güell in the Sagrada Família Museum (Canaan, 2009).

The method uses two diagrams to solve axial loads in elements of a structure. Using a method similar to the triangle of forces drawn for the object in equilibrium shown in fig. 6, the axial forces in the elements of a truss can be calculated.

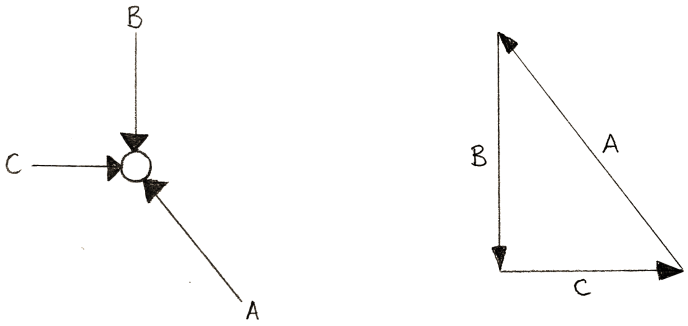

Figure 6. An object in equilibrium (left) and the corresponding triangle of forces (right)

The first diagram – the *form diagram* – shows the position and direction of the lines of action of the structural members, the second – the *force diagram* – shows the direction and magnitude of the forces carried by the elements of the form diagram. The does not take into account moments or deflection, and cannot calculate shear forces or bending moments developed in the elements. Typically it is used to solve problems in 2D structures but it is possible, although difficult, to calculate in 3D (Van Mele et al., 2012). The full method will not be described here, but various books are available on the subject, such as Allen and Zalewski's *Form and Forces: Designing Efficient, Expressive Structures* (2009).

5. The Clifton Suspension Bridge

5.1. The history of the bridge

The story of the Clifton Suspension Bridge started more than 100 years before the opening of the bridge, when in 1754 William Vick, a local merchant, bequeathed £1,000 for the building of a stone bridge over the Avon Gorge between Clifton Down in Gloucester and Leigh Woods in Somerset (McIlwain, 1996). By 1829 the legacy was worth £8,000 but the estimated cost of a stone bridge was around £90,000, so a competition to design a suspension bridge was announced (McIlwain, 1996). Twenty-two entries were received, including one from Brown, the designer of the Union Chain Bridge, and four from engineer Isambard Kingdom Brunel. Thomas Telford was appointed to select a final design, but rejected all of them and submitted his own design (Body, 1976).

Telford's design had three spans and was supported by two towers in a gothic revival style. He maintained that 183m was the greatest admissible span. However his design was heavily criticised by the public, and so a second competition was held in 1830. Brunel's plans were rejected again, however he arranged a meeting with the judges and convinced them to accept his design with the towers decorated in an Egyptian style. Having raised over £32,000 of the £57,000 total estimated cost, work began in 1831 (Body, 1976; McIlwain, 1996). The project was plagued by delays, disputes and financial difficulties and by 1843 only the abutments and towers had been built, at a total cost of £45,000. The main contractor went bankrupt and the project was abandoned (McIlwain, 1996).

Brunel's death in 1859 brought about renewed interest in the project. Engineers John Hawkshaw and William Barlow formed the Clifton Suspension Bridge Company in 1861 and work was resumed in 1862 (McIlwain, 1996). It was decided to use the chains from Brunel's Hungerford Bridge, London, which had recently been demolished. Various modifications were made to the original design; increasing the number of suspension chains from two to three; the design of the towers was simplified and their height increased by 5m; the chain-anchorages were brought nearer; the wooden deck girders were replaced with iron and, using Arnodin's recent improvements to deck design, the parapet was used to stiffen the longitudinal girder (Barlow and Ben, 2003). Work was completed in 1864 and to test the bridge, 500 tons (508023kg) of stone was evenly distributed across the deck, producing a deflection of only 180mm (Barlow and Ben, 2003).

Since then the opening of the bridge, little about the design has changed. The wooden deck was first asphalted in 1897 (Cullimore, 1986). In 1925 extensive reinforcement of the chain anchorage was carried out (Body, 1976) and in 1953 a maintenance frame was added and the modern vehicle weight limit of 4 tons (4064kg) was introduced. The timber deck has been replaced on several occasions and the metalwork has been grit-blasted and zinc-sprayed to reduce corrosion (Cullimore, 1986).

More recently, in 2003, the bridge became overloaded with crowds for the Ashton Court Festival and the Bristol International Balloon Fiesta. Since then, the bridge has remained closed on these days to prevent damage to the structure ("Suspension bridge shut for events," 2005). In 2014, the bridge was closed for the first time due to high winds ("High winds force closure of Bristol's Clifton Suspension Bridge," 2014).

Although not completed until the 1860s, the Clifton Suspension Bridge is a valuable example of early British suspension bridge design. Its iron chains, wooden deck and longitudinal plate girder make it one of a few remaining examples, including the Menai bridge and the Union Chain bridge.

5.2. Analysis of existing documentation and description of bridge

The information in this paper comes from several distinct sources; Barlow's 1867 paper, *A Description of the Clifton Suspension Bridge*; various plans held by the Clifton Suspension Bridge Trust and *The Clifton Suspension Bridge: preservation for utilisation*, by Cullimore, 1986. Brunel's original sketches and calculations are held in the Brunel Institute, but the modifications made by Barlow and Hawkshaw make them of little value for the purposes of calculations.

A Description of Clifton Suspension Bridge contains the dimensions of the bridge; diagrams of the bridge profile and a section of the deck; notes on the construction method and calculations for the maximum stress developed in the chains and hangers. It provides an almost complete description of the bridge. Having been published before the introduction of SI units and standard nomenclature, all measurements are in imperial units. More notable is the Barlow's discrepant terminology; he writes that 'The strain…. at the centre of the chains is 597 tons approximately,' but goes on to write in the next paragraph that 'the maximum strain upon the iron is….4.76 tons per square inch'. It can be assumed in this case that 'the strain' refers to axial load and stress respectively. However, at other times the information is meaningless: 'the suspension-rods are each rather more than 2 inches in section.' For this reason, information from Barlow's paper is only used when it agrees with that of another source.

In *The Clifton Suspension Bridge: preservation for utilisation*, Cullimore describes the results of fatigue and fracture testing in the deck and hangers as well as details of operational practice and maintenance.

Figure 7. The southern side of the Clifton Suspension Bridge with Avon Gorge in the background. The Leigh Woods tower (left) has a different design to that of the Clifton tower (Gothick, 2009).

According to the description given by Barlow and Ben (2003), the Clifton Bridge is a single-span, eyebar-chain suspension bridge. It has three chains on either side of the roadway which each chain supports a plate girder longitudinally along the bridge by means of 81 vertical hangers. Directly below each hanger the longitudinal girders are connected by

transversal open lattice girders that are riveted to the lower flange of the longitudinal girders, and diagonal cross bracing that is bolted to the underside of the deck timbers. The area between the two longitudinal girders is the carriageway and the cantilever sections of the transversal girders support the pedestrian walkway and the parapet. The parapet is a lattice girder and works to increase the longitudinal stiffness of the deck. The chains, hangers, girders and parapet are all made of wrought iron. Rather than passing continuously over the tower saddles – as is common in more modern suspension bridges – the suspension chains and land chains are attached directly to a frame on cast iron rollers.

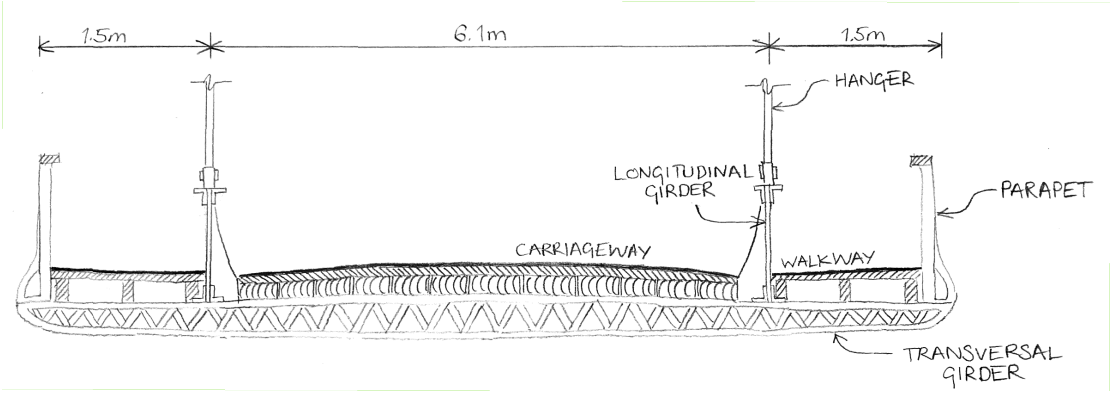

Figure 8. Section through the deck. Not to scale.

The 26m (85ft) towers are made of local sandstone (Cullimore, 1986) and are positioned 214m (702ft) apart, while the suspended section of the roadway is only 193.9m (636ft) long (Barlow and Ben, 2003). Barlow and Ben (2003) write that along the suspended section, there is a transversal girder and hangers every 2.4m (7.95ft). In the centre of the bridge, the chains are 21.3m (70ft) lower than at the towers. The distance between the two sets of chains width of the carriageway is 6.1m (20ft) – one 3m wide lane of traffic in each direction. Each walkway is 1.5m (5ft) wide. The Clifton side of the bridge is 0.9m (3ft) higher than the Leigh Woods side, something that Brunel believed would make the bridge appear absolutely level against the backdrop of the gorge. The deck is slightly cambered, so that the centre is 0.61m (2ft) higher than at the ends.

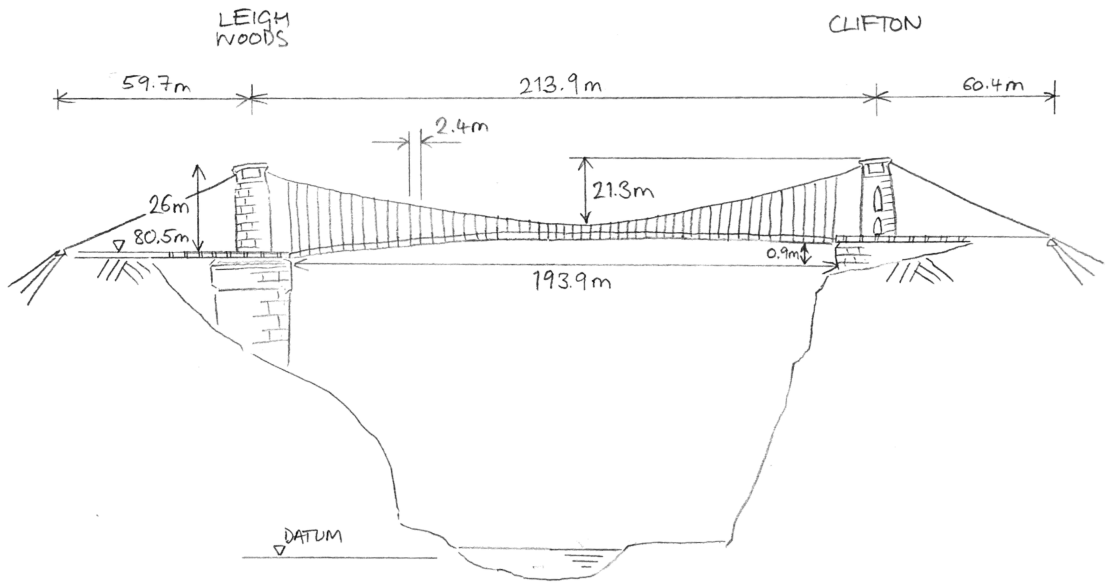

Figure 9. Diagram of the southern view of the bridge. Not to scale.

The deck is made of 127mm deep timber planking laid longitudinally across the transversal trusses and covered with a layer of 50mm thick transversal planking. The surface is finished with 32mm nominal thickness mastic asphalt (Cullimore, 1986).

Figure 10. Photograph of the Leigh Woods tower with the land chains in the foreground (D, 2007).

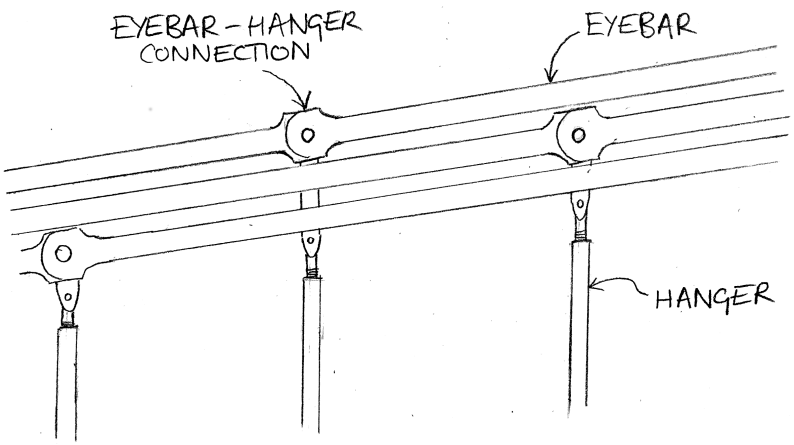

Figure 11. Detail of the suspension chains, showing the arrangement of the hangers and eyebars.

5.3 Structural analysis

In the following section, the chain and the transversal girders have been analysed using a numerical method (a computer model analysed in the program SAP2000) and a graphical method (graphic statics). This permits a critical evaluation of the design of the structure and a comparison between said analytical methods with regards to their accuracy, ease of use and relative power.

5.3.1 Transversal girders

5.3.1.1. Model

A simplified model of the transversal girders has been used for the analysis. It comprises a top and bottom boom, each made of two 100×100×16 angles back-to-back with flat bar diagonal bracing sandwiched between the two (see figure 12). It is simply supported at the two nodes that correspond to the connections with the longitudinal beams and all applied loads act within the plane of the girder. The material is assumed to be uniform wrought iron

with a density, ρ of 7750kg/m^3 (Shackelford et al., 2016). Details such as bolts and rivets have not been taken into account.

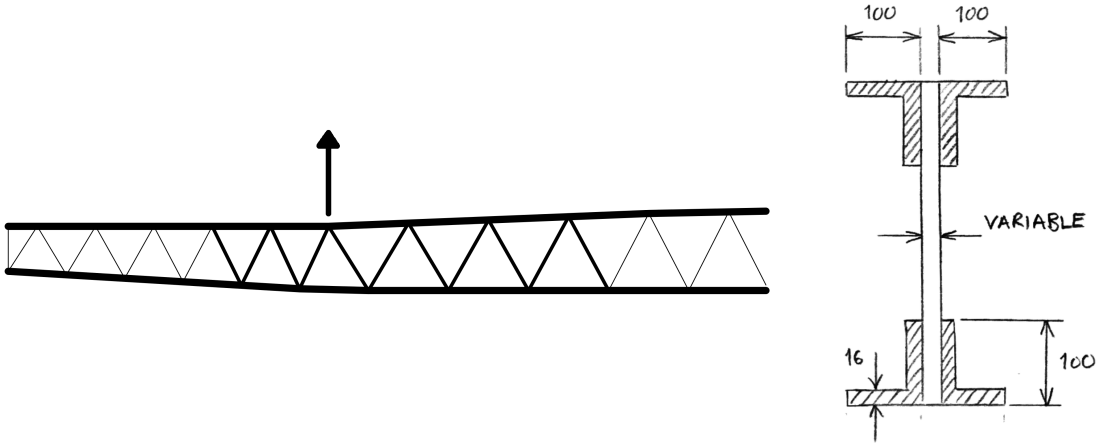

Scale elevation of half of the girder. Cross section. Not to scale.

Figure 12. Approximation of the transversal girder as used in the analysis.

5.3.1.2. Loading

The loads applied to the model are divided into the categories. The self-weight of the girder, the superimposed dead load – the weight of the deck and the parapet – and the live load. In the numerical method, the self weight of the elements is calculated from their volumes and the specific weight of the material. In the graphical method the self weight has not been taken into account.

The superimposed dead loads have been calculated as follows assuming the deck composition shown in figure 13 and that the girder supports a section of deck 7.95ft (2.4m) long (see figure 14). The densities of the timber and the asphalt are taken as 530kg/m^3 and 2300kg/m^3 respectively (Richards, 2010).

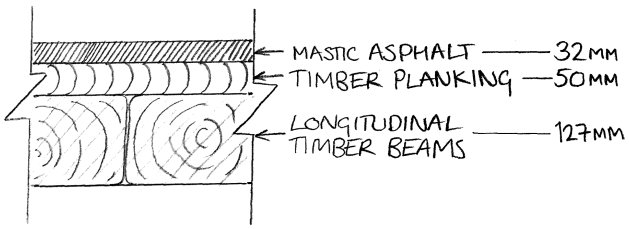

Figure 13. Section through the roadway. The walkway is assumed to be the same but without the bottom layer.

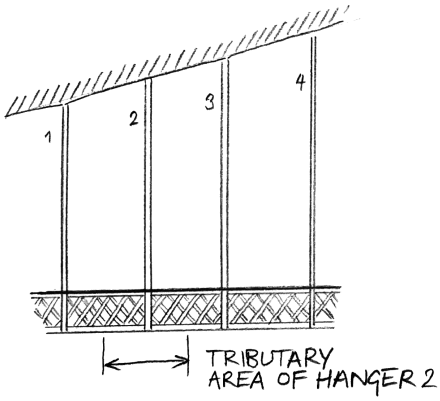

Figure 14. The tributary area of each hanger is 7.95ft (2.4m) long.

Four combinations of live loads have been used in order to find the most unfavourable combination of loads. One is based on Barlow's estimated maximum live load of 70lbs per square foot (3.35kN/m^2) distributed uniformly over the whole deck. The other load cases are to reflect the maximum loading that occurs today. The maximum live load on the pedestrian walkways is assumed to be 5kN/m^2, in accordance with *EN 1991-1-1* (British

Standards Institution, 2002) for areas susceptible to crowds and *IAP-11* (Ministerio de Fomento, 2011) for pedestrian loads on road bridges. European standards are not valid for the loading on the carriageway as a 4 ton vehicle weight limit is enforced. Therefore a uniformly distributed load of 2.65kN/m^2 has been calculated assuming a 4 ton vehicle situated every 5m along the deck in both lanes. The automatic toll barriers regulate the flow of vehicles across the bridge (Body, 1976), so this value is conservative.

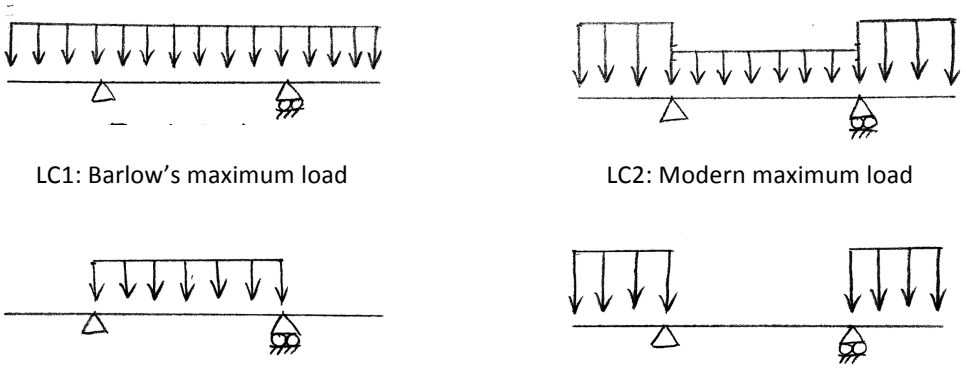

LC1: Barlow's maximum load LC2: Modern maximum load

LC3: Load to produce maximum sagging of girder LC4: Load to produce maximum hogging of girder

Figure 15. The four load combinations (LC) used in the analysis.

The dead loads are multiplied by a coefficient of 1.35 and the live loads by 1.5 to account for underestimates of the maximum loads – providing a so-called *factor of safety*. The coefficients are applied in all cases except LC1, so as to compare the results with the calculations made by in *A Description of the Clifton Suspension Bridge*.

5.3.1.3.Results of numerical method

For all of the load cases, the axial load in each element was recorded. For the purposes of this paper, an element refers to linear member between two nodes in the model. For example, the top boom is a single object composed of 28 elements of different lengths and a piece of bracing is a single element. Figures 16—19 show the axial load envelopes of the booms and bracing of the girder. It should be noted that while the diagrams of the booms show the load in a single object, the diagrams of the cross bracing show the axial load many individual objects.

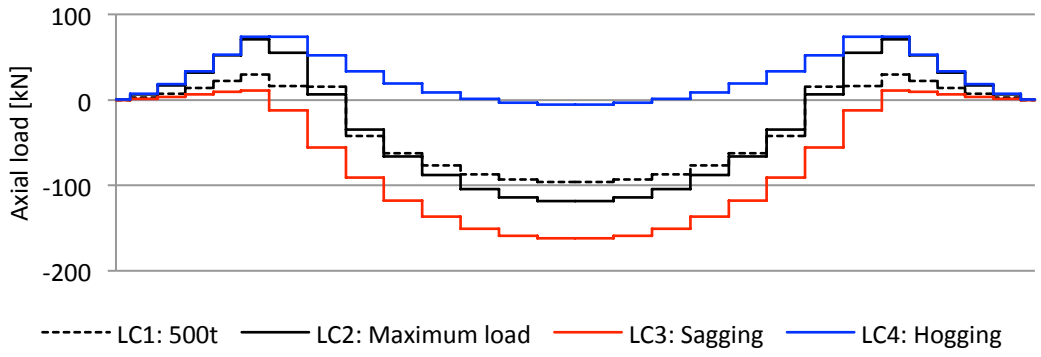

Figure 16. Axial force envelope for the top boom. The greatest tensile load (74.0kN) occurs during LC4 and the greatest compressive load (162.0kN) during LC3.

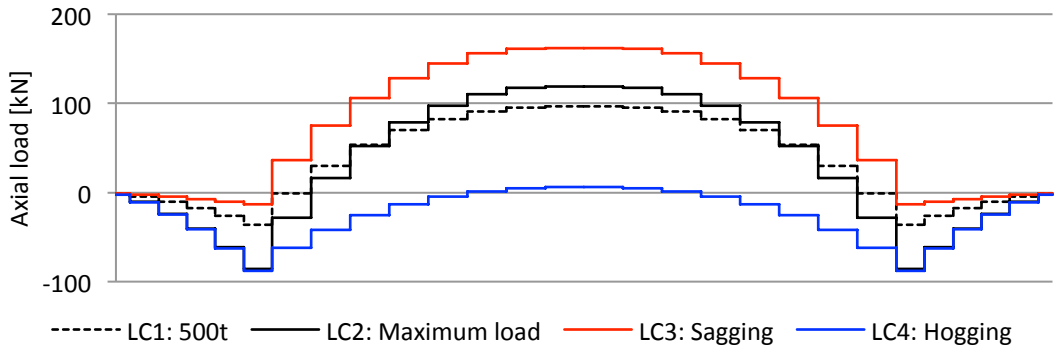

Figure 17. Axial force envelope for the bottom boom. The greatest tensile load (162.4kN) occurs during LC3 and the greatest compressive load (88.3kN) during LC4.

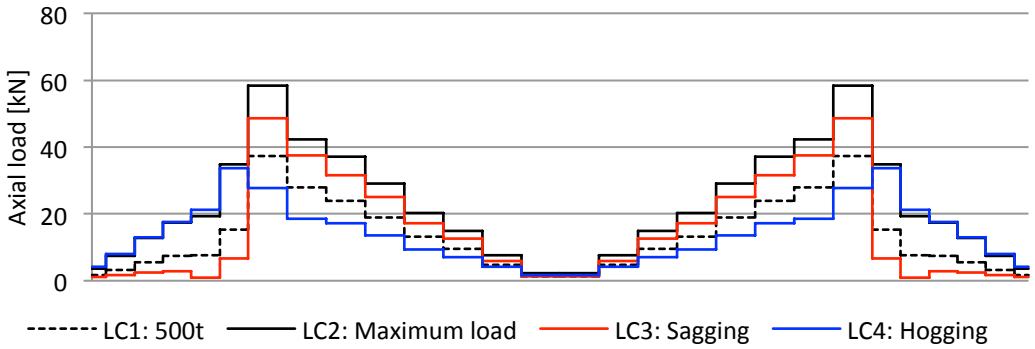

Figure 18. Axial force envelope for the tension bracing as seen in Figure 12. Approximation of the transversal girder as used in the analysis.

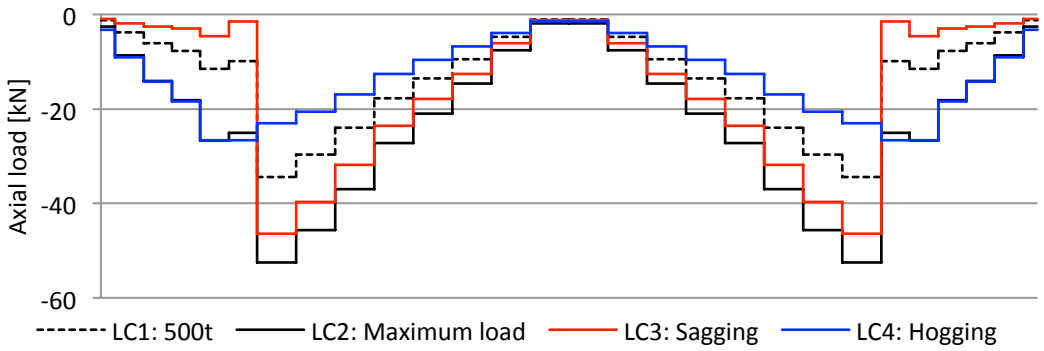

Figure 19. Axial force envelope for compression bracing as seen in figure 12.

The greatest load in the booms is found in the centre of the span, where the girder is deepest. Axial force in the booms is primarily caused by bending, so it is good to note that the envelopes in figures 16 and 17 closely resemble the bending moment graphs of a simply supported beam subjected to a uniformly distributed load – the greatest bending moment is found in the middle of the span. The same observation can be made in figures 18 and 19, where the greatest axial loads in the bracing occur at the connections with the longitudinal girders; when girder is seen as a simply supported beam, the shear force diagram peaks where the reaction forces are applied to the beam.

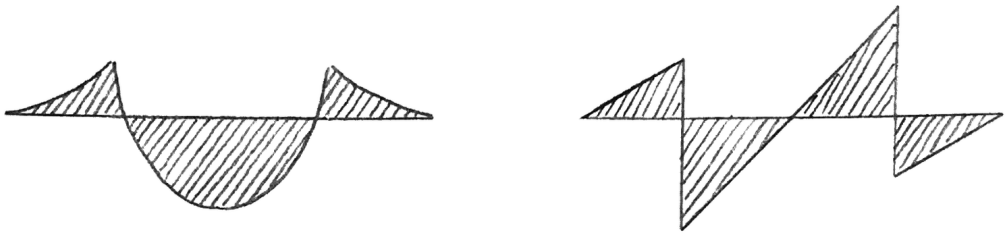

Figure 20. The distribution of bending moments (left) and shear forces (right) in a simply-supported beam with a uniformly distributed load.

With these results, the critical element and of the girder can be calculated – that is the element that will fail first in the case that the beam is overloaded. There are no modern guidelines for the use of wrought iron in structural design, so the calculations were using the method in EN 1993-1-1 (British Standards Institution, 2005) and material properties of wrought iron as listed in ASTM A207 (ASTM International, 1939); the ultimate tensile strength (UTS) is taken to be 330kN and the yield strength, f_y as 190kN. To account for imperfections in the material, the UTS and f_y are divided by a reduction coefficient of 1.15.

The critical tensile load, N_{cr} and the flexional buckling load $N_{b,Rd}$ were calculated for the top and bottom booms and the critical bracing elements. There are two sizes of bracing, as shown in figure 21, so loads have been calculated for both.

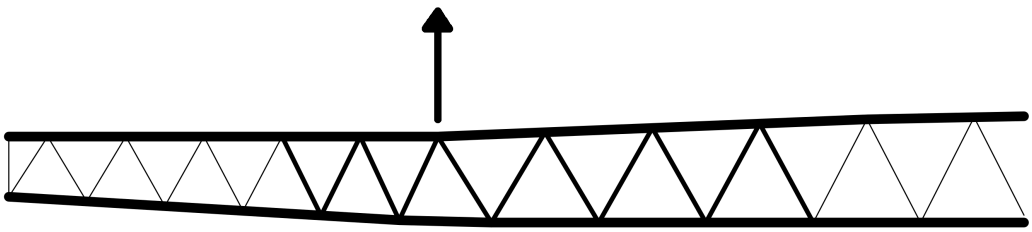

Figure 21. The girder bracing is made of two sizes of flat section. The light elements have sections of 2”×3/8” (50×10mm) and the dark elements 2”×0.5” (50×13mm) sections.

Table 1. Calculation of the critical tensile load for each element type.

Object	Top boom	Bottom boom	2”×0.5” bracing	2”×3/8” bracing
Section area, A [mm]	5888	5888	806	605
Tensile load, T [kN]	73.9	162.4	58.3	20.3
Stress, σ [MPa]	12.6	27.6	72.3	33.6
Critical load, N_{cr} [kN]	1689.6	1689.6	231.4	173.6
Factor of safety, F	22.8	10.4	4.0	8.5

The factor of safety, F is the ratio N_{cr}/T. If $N_{cr} \gg T$, the value of F is high and suggests an inefficient use of material. If $F < 1$, the element is not strong enough and will fail during normal use. The results of the analysis show that all the sections have a sufficient factor of safety and that the girder appears to be inefficiently designed for tensile loads. The 2”×0.5” section has the lowest factor of safety, which suggests that it would be the first to undergo tensile failure if the loads were further increased.

To calculate the compressive capacity of each section, the buckling load $N_{b,Rd}$ was calculated. All the elements are slender ($\lambda > 0.2$) so will fail in buckling and not crushing. To make the calculation, it was assumed that all the elements were fixed at both ends. This means the effective length, $L_e = 0.7 \times L$, where L is the actual length of the compressed section. The top boom is bolted to the longitudinal deck timbers, effectively reducing the unconstrained length, however this is not taken into account.

Table 2. Calculation of the flexional buckling load for each element type.

Object	Top boom	Bottom boom	2”×0.5” bracing	2”×3/8” bracing
Compressive load, C [kN]	162.0	88.2	52.5	27.2
Stress, σ [MPa]	27.5	15.0	65.1	44.9
Moment of inertia [mm^4]	2834350.3	2834350.3	10839.4	4572.9
Effective length [mm]	4267	4267	186	206
Non-dimensional slenderness, λ	2.0	2.0	0.7	1.1
Flexional buckling load, $N_{b,Rd}$ [kN]	233.2	233.2	116.5	59.9
Factor of safety, F	1.4	2.6	2.2	2.2

The results show that the sections are much more efficient in compression than in tension. The critical section is the top boom, which agrees with the findings of the test to destruction, where failure occurred due to buckling of the top boom. However the calculated buckling load is likely to be conservative, as Cullimore (1986) notes that longitudinal deck timbers have a considerable stiffening effect on the girder. He also writes that there was visible bowing of the bracing and bottom boom, suggesting that they have a similar factor of safety. This agrees with the results of the calculations as seen in table 2.

5.3.1.4. Calculation with graphic statics

As the girder and the load cases are both symmetrical, and the graphic statics method does not take into account moments of any kind, it is only necessary to analyse half the truss, as shown in Fig. 22. To emulate the graphic statics as it would have been done in the 19th century, all the graphic analysis was drawn by hand on A0 paper. This permitted precision of up to 0.5kN, when using measurements in millimetres and a scale where 10kN is equal to 1cm. The analysis was repeated using computer-aided design (CAD) software, so that the error resulting from the hand drawings could be calculated.

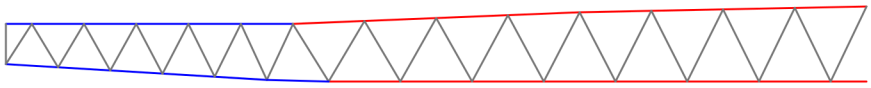

Figure 22. Half of the girder model, as analysed with the graphic statics. The sections of the booms under the walkway are blue and those under the carriageway are red. The cross bracing is in grey.

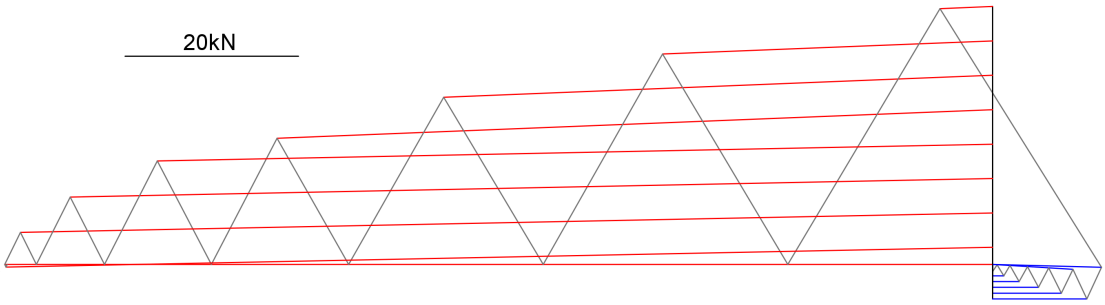

Figure 23. CAD force diagram of the sagging load case. The vertical black line represents the total load upon the girder. The forces in the top and bottom boom where they pass under the walkway (blue lines) are insignificant in comparison to where they pass under the carriageway (red lines).

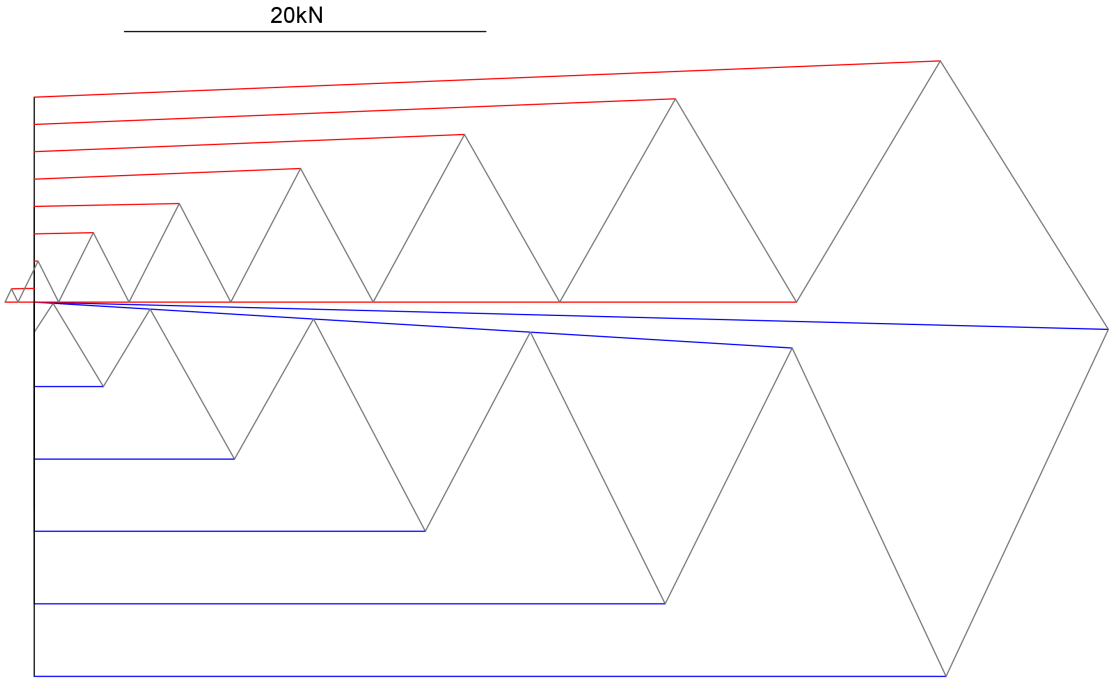

Figure 24. Force diagram of the hogging load case. The vertical black line represents the total load upon the girder. The maximum axial forces of the sections below the walkway and carriageway are of similar magnitudes and less than half that of the maximum force in fig. 23.

The results of the hand-drawn graphic statics were compared to those found using the CAD drawings. The mean error for the four load cases was 0.3kN and the maximum error was found to be 3.1kN. As the theoretical precision of the hand-drawing is 0.05kN at a scale of 1kN:1cm, this method was not accurate. However for the purposes of structural engineering, where loads are often calculated to the nearest 1kN, it could be considered to be accurate. However it is worth noting that average percentage error of the drawings was 8%. Small values, especially those less than 1kN are more sensitive to the effects of the error.

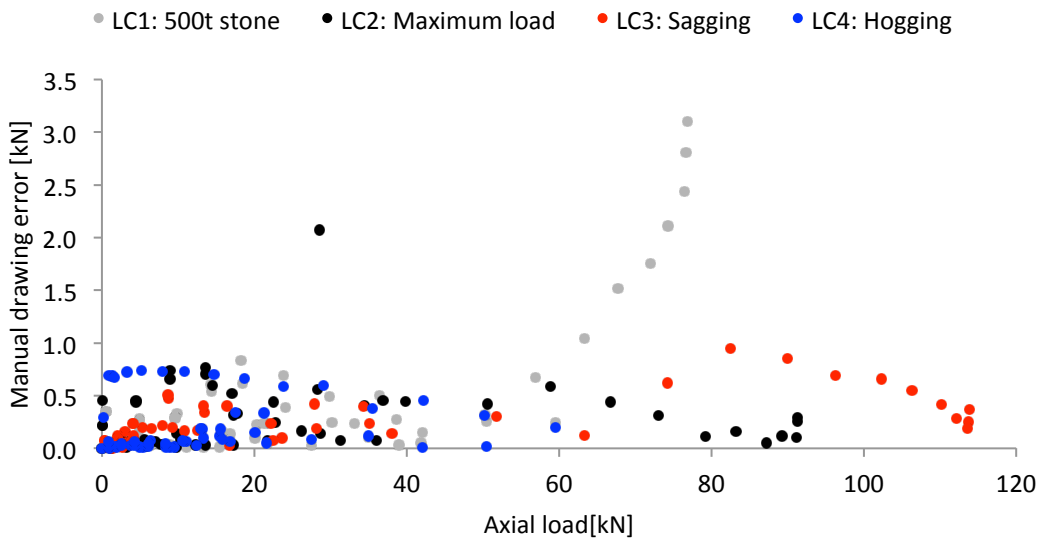

Figure 25. Graph showing the absolute manual drawing error against the axial loads in each member.

As seen in figure 25, the majority of error is less than 1kN, however the results for LC1 display some unusual characteristics. For axial loads greater than 60kN, the error increases rapidly with axial load, with a maximum of 3.1kN. This is fundamentally an effect of the graphic statics method, where the positions of joints are found from the intersection of lines of force. Any error in finding the intersection will be carried over into the calculation of the length of the next force line to be calculated. The longer the line, the more the error is amplified; so small errors at the beginning of the process can lead to a chain-reaction that causes larger errors later. It is possible that the effects of this phenomenon can be reduced by calculating the largest values in the structure first, however it has not been investigated for this project.

5.3.1.5. Comparison of graphic statics and numerical method

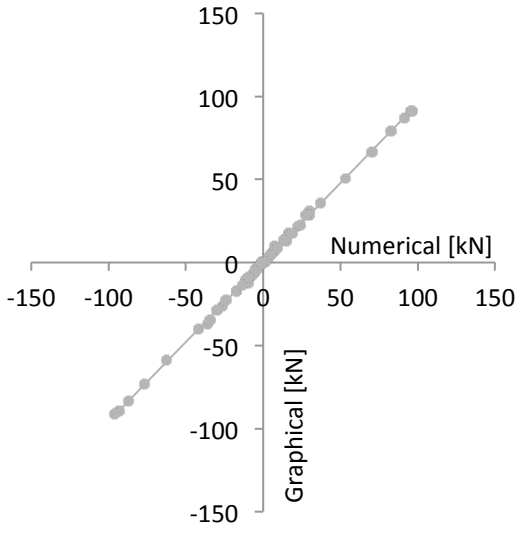

LC1: Barlow's load. r^2=0.999. Gradient of trend line = 0.9571

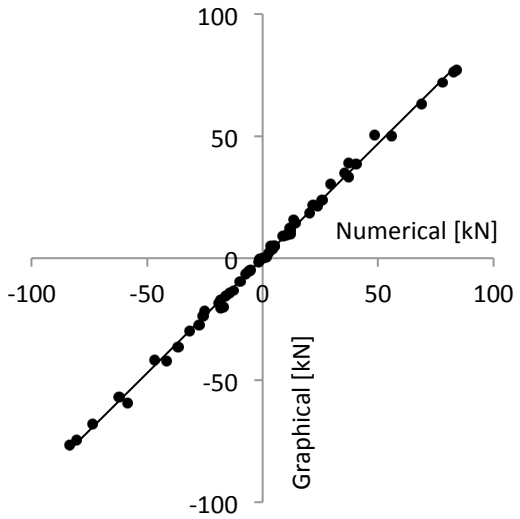

LC2: Maximum load. r^2=0.997. Gradient of trend line = 0.94.

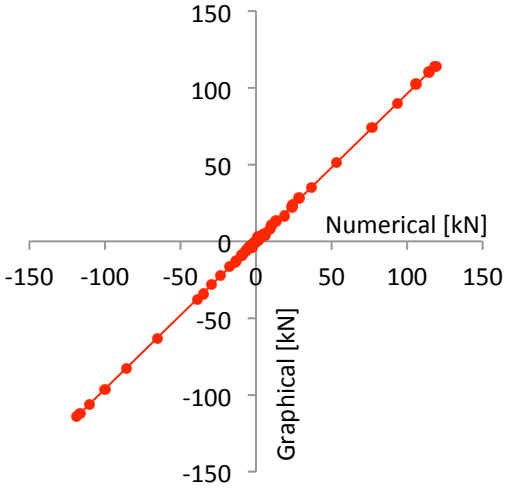

LC3: Sagging load. r^2=1.000. Gradient of trend line = 0.9623.

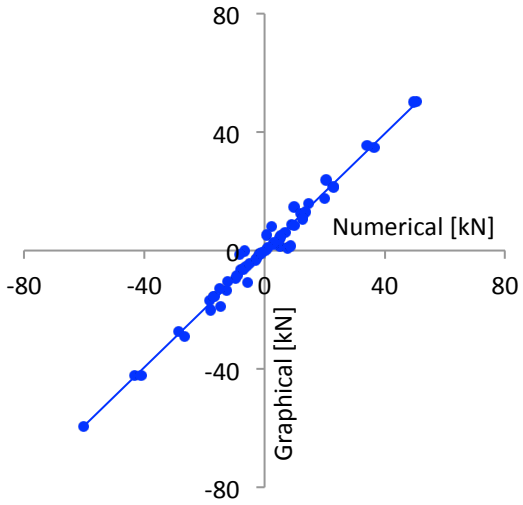

LC4: Hogging load. r^2=0.982. Gradient of trend line = 0.9867.

Figure 26. Loads obtained from the CAD drawing method against those obtained from the numerical method, for each load combination. The r^2 value shows the correlation between the results.

A comparison of the results from the numerical and graphical analysis shows a very strong linear correlation (see fig. 26). It is not completely certain what causes the slight error between the results. There is assumed to be no error in the CAD drawing nor in the results of the numerical analysis, and the data was recorded to the nearest newton. It is partly caused by the difference in the models; graphic statics assumes that all joints are pins, so no moments are transferred between elements. During the numerical analysis the elements in the booms were calculated with fixed ends, as each boom is a single object. To measure the effect of this difference, the numerical analysis was repeated with a completely pinned structure.

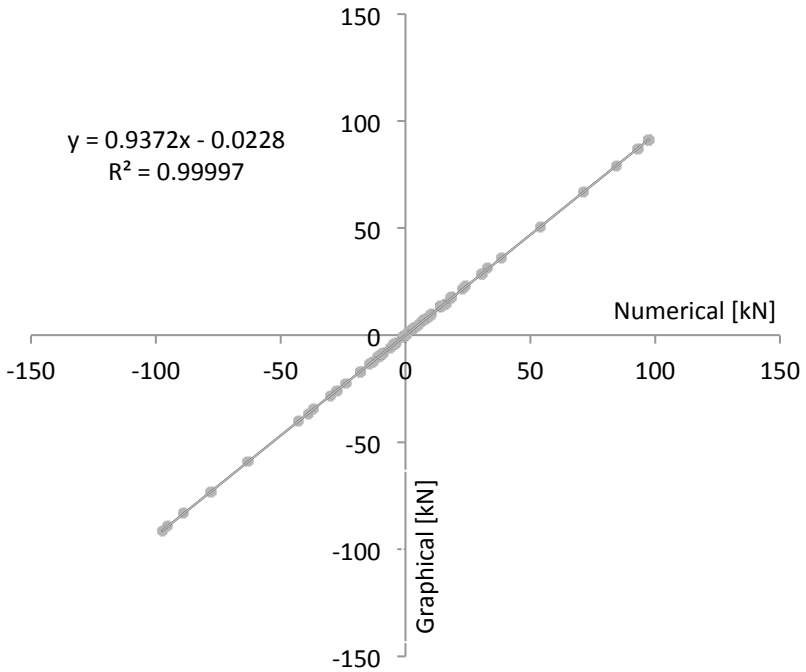

Figure 27. Graph of axial loads calculated with CAD drawing and those of the numerical analysis of the completely pinned girder for LC1. r^2 = 0.99997.

Fig. 27 shows that there is a nearly perfect linear relationship between the results, which suggests that the disparity between the models is the primary cause of the error in the results. It is unknown whether the geometry and type of loading has an effect on the fixed–pinned difference, but it is not investigated in the paper.

In all cases, the results of the graphical analysis are less than that of the numerical one. Although the results are proportional, they are not equal; the trend lines show that the loads found using graphic statics are 94-99% of those of the numerical analysis. The difference is that of the self-weight of the girder, which has not been taken into account in the graphical analysis.

Based on these observations, the graphical method of analysis can be seen as a valid and useful alternative to numerical analysis. It has limited uses (being only able to analyse axial loads on statically determinate structures with pinned joints) and is inaccurate and highly time consuming when done by hand. However, in this case where a high level of precision is not required, it provides sufficient data to be able to calculate the behaviour of the structure. The drawings themselves may be seen as a useful way to visualise the behaviour of the structure, and could provide students of engineering an alternative way to learn about structural mechanics and analysis. It is interesting to note that these graphical methods went out of use as mathematical modelling became more sophisticated, at a time when engineers were 'blindly trusting of results' (Gimsing, 1984). It should be asked whether graphical methods, although antiquated, help give an innate understanding of structures that modern engineers no longer have.

5.3.2. Chains

Knowing the geometry of and the loads applied to a structure allows the forces inside to be solved with graphic statics, as previously described. The nature of graphic statics means that the geometry of structures can be ascertained if the forces within the structure are known. This can be used to calculate the shape of a hanging cable, or – in the case of the Clifton bridge – the optimal shape of the suspension chain. The optimal shape of a cable is that in which the loads in the cable are minimised. In cases where the self-weight of the cable is insignificant, that shape is a parabola. Although the chains of the suspension bridge are made of discrete links and have significant self-weight – approximately 1/3 of the total load (Barlow and Ben, 2003) – the shape can still be approximated to a parabolic curve.

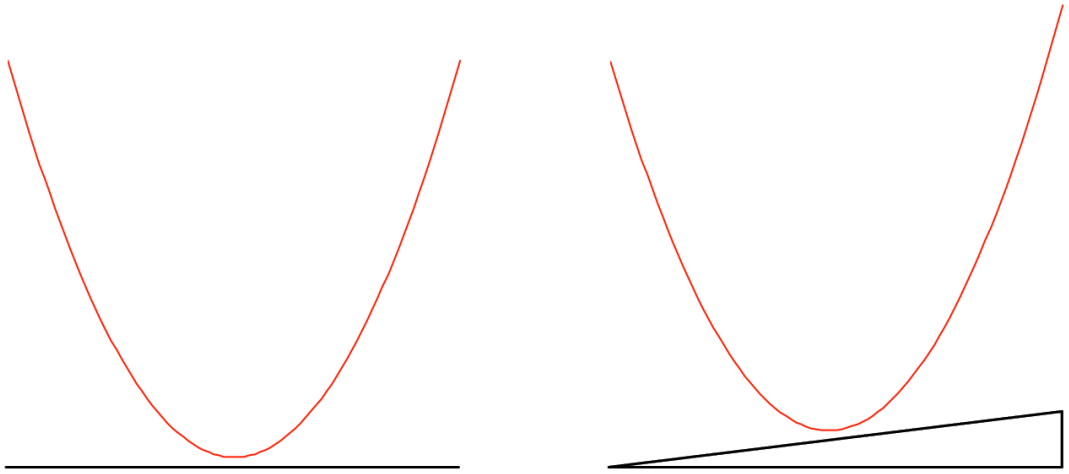

Figure 28. The shape of the chain if it were to hang between towers of equal heights is a parabola (left). The same shape adjusted by increasing the levels linearly along its length –no longer a parabola (right). Not to scale.

The calculation of the shape of the Clifton bridge is complicated by the fact that the Leigh Woods tower is 3ft (0.9m) lower than the Clifton tower, giving the bridge an average

gradient of 1:233 (Barlow and Ben, 2003). It appears that the shape of the Clifton chains was calculated by taking the shape of a parabola with level ends and then increasing the levels linearly along the length of the chain, as illustrated in fig. 28. McIlwain (1996) writes that the design was 'close to the ideal', suggesting that this method is not accurate but makes a good approximation to the optimal shape. Using graphic statics and the structural analysis program SAP2000, it was possible to analyse the shape of the chain.

Barlow and Ben (2003) calculate the maximum load in the chains to be 2094 tons-force (21,276kN), approximately 10,638kN in each set of chains. Using the detailed information provided by Cullimore (1986), it is possible to make our own estimate to the maximum load in the chains between the towers.

Table 3. Weights and loads for half of the deck, to calculate the load in one set of chains. The chain weight is that of a parabolic shape chain. Other ironwork refers to longitudinal and transversal girders, hangers and parapet.

Load	Estimated value
Self-weight of 1 set of chains	2761kN
Self-weight of other ironwork	903kN
Super-imposed dead load	1290kN
Live load (LC1: 70lbs/sq. inch)	3070kN
Total	8024kN

The maximum axial load of a uniformly loaded light cable, T_{max} can be calculated using equation 1, where ω is the uniformly distributed load, L is the length of the chord and h the height of the curve.

$$T_{max} = \sqrt{\frac{\omega^2 L^2}{4} + \left(\frac{\omega L^2}{8h}\right)^2} \quad (1)$$

The calculated T_{max} is 11,100kN, which is approximately 4% greater than Barlow's estimated maximum. This is sufficiently accurate to be used in the calculations of the shape of the chain.

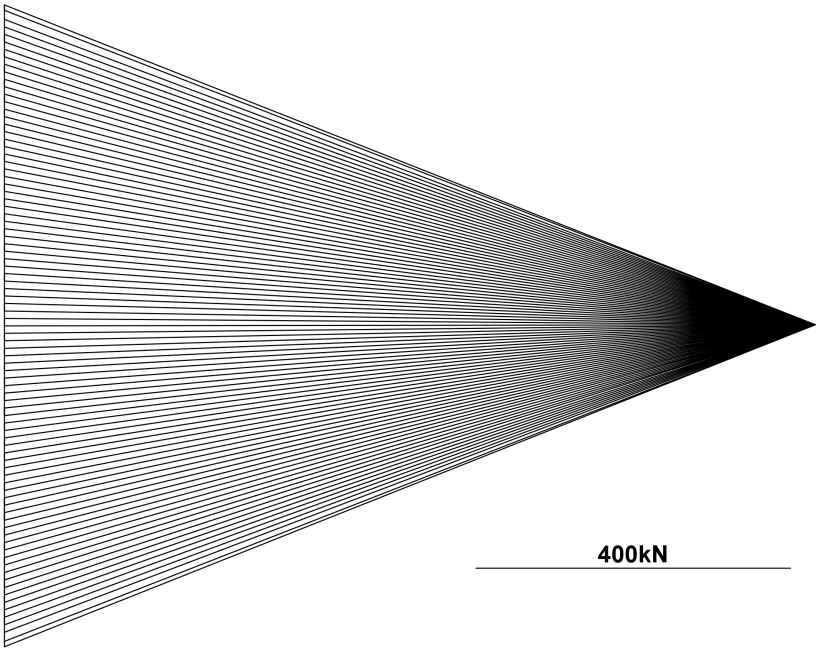

Figure 29. Force diagram of one set of chains (supporting half the deck) with uniform live loading across the deck.

Having verified the Barlow and Ben's figures, the force diagram in fig. 29 was created. The length of the vertical line represents the total magnitude of the load on the chains; each small vertical line, the load transferred to the chains by one hanger. Each of the convergent lines is the load in one section of the chains. The average gradient of these lines is 1:233. This means that the diagram is not symmetrical and the bottom line is longer than the top. It represents the force in the section of the chain with the greatest load 11,100kN. Knowing this value, it is possible to create the entire force diagram.

The shape of the chain can now be calculated, as the gradient of each chain section is known.

5.3.2.1. Chain Shape

As shown in fig. 30, the optimal shape as calculated with graphic statics does not agree with the real shape of the chain. There is a maximum difference of 2.6ft (0.79m) between the graphic statics curve and the real shape of the chain. The disparity is caused by the fact that the theoretical chain shapes have been calculated for a chain in which the maximum load is that 11,100kN, as mentioned above. To create a shallower curve, the maximum load in the chain would have to be increased. It may be that the chain shape was designed with a slightly higher maximum load as a precaution.

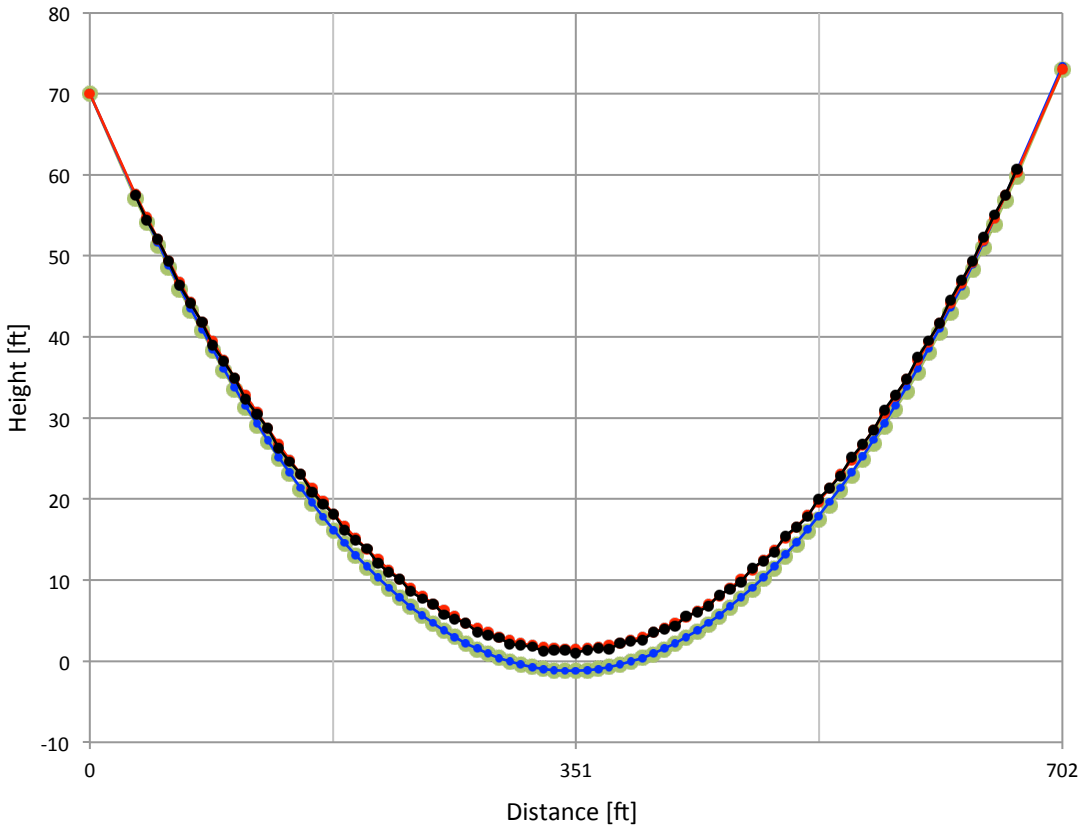

Figure 30. The shape of the chain calculated with graphic statics (blue), the adjusted parabola shape shown in fig. 28. (red), the actual chain shape (black) and the shape calculated in SAP (green). The chain shape is known from the measured lengths of the hangers, so is only shown for the suspended section of the bridge. Heights are relative to the original parabola similar to that in fig. 28.

In figure 31, the results are compared to a parabola 702ft wide and 70ft deep, which are the approximate dimensions used in equation 1. It is easy to see that the chain as-built is very similar to the 'adjusted parabola' in fig. 28. The slight deviation is probably due to the

wearing of the eyebars and deflection of the chains. The methods used here are based on first-order static theories and do not calculate the deflected shape as in second-order theories. There is considerable error in the hand-drawn graphic static method – it increases towards the centre of the span the until it is 0.9ft (0.27m). However it then decreases again on the other side, so that the magnitude of the error is symmetrical across the centre of the span. This suggests that the cause is not random measuring error, but an error in the force diagram. The curves of the CAD graphic statics and the cable produced by the numerical method are very similar, which suggests that the methods have been carried out correctly. The effect of the UDL in comparison to the loads calculated in the graphic statics is small, the chain shape under the UDL is slightly shallower, however by only 0.2ft (6cm).

The results from the numerical and graphical analysis create curves that have their minimums closer to the lower tower than the upper. Unlike the shape in fig. 28 that closely resembles the actual chain shape, the curves have been effectively moved horizontally towards the lower tower. This is what is expected and closely resembles the optimal shape for the chain.

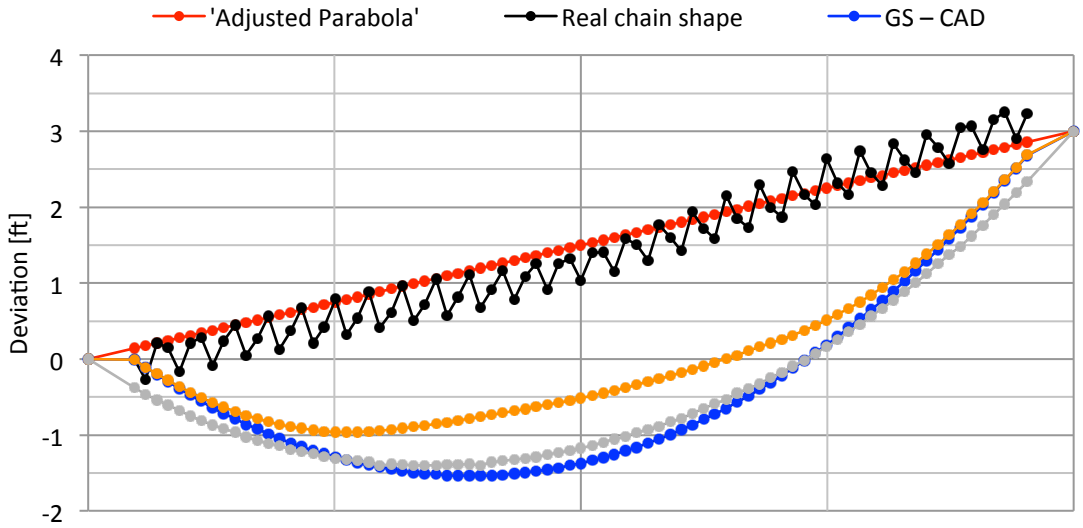

Figure 31. Deviation of curves from original parabola, as shown in fig. 28. The series of black points are the levels of the upper hanger connections, which are attached to each of the three levels of chains alternately along the length of the chain (see fig. 11).

The analysis of the chain shape was done using the loads calculated for LC1 – Barlow's original design loads. However it should remain valid for the other load combinations because the shape found is dependant on the distribution of the loads along the length of the structure, not the total load itself. For this reason it can be assumed that the result of the same calculation with different loads would be similar – the optimal chain shape today should not be different to that of the 1864.

However it is important to note that this may not be the most unfavourable load combination for a chain of this shape. Loads that are distributed unequally along the length of the bridge might cause greater forces in the chain, because the chain shape would no longer be optimum for this loading scenario.

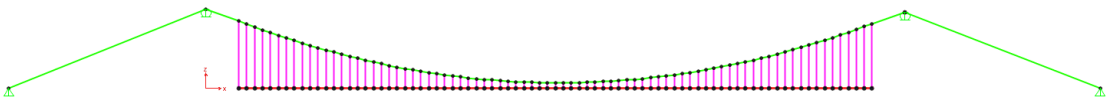

Figure 32. Longitudinal model of the bridge, as constructed in SAP2000.

Using the dimensions detailed earlier, a simplified 2D model of the bridge (see fig. 32) was analysed in SAP2000 to see what the effect of non-uniform loading along the length of the bridge would have. The model comprises one set of chains with a cross-sectional area of 220 square inches (141935mm^2) – the minimum area (Barlow and Ben, 2003). The set of chains is connected to single longitudinal I-beam 3ft (0.91m) in depth by cylindrical hangers with diameters of 47mm (Cullimore, 1986). The chains are connected to fixed restraints at the land anchors and rollers at the towers. The longitudinal beam is simply supported at each and all the hangers are pinned. The same wrought iron material as described above is used throughout. During the analysis, point loads were applied at each of the nodes connecting the hangers and the longitudinal beam to simulate the live load and the dead load contributed by the deck. The results of the analysis are shown in table 4.

Table 4. Results of the SAP analysis.

Live load	Full length	Half length
Maximum reaction at tower saddles [kN]	8262	7931
Maximum load in chain [kN]	11013	10550
Minimum load in chain [kN]	10345	9910
Max. bending moment in longitudinal girder [kNm]	300	2208
Maximum vertical deflection of deck [m]	0.35	4.05

There is little difference between the two combinations of loads in terms of the load transmitted through the chains and towers. The loads in the chain and the reactions at the towers for the half-length load are approximately 5% less than those of the full-length load. This suggests that while the half-length load is transmitted less efficiently through the structure, the full-length load is still the most unfavourable in terms of axial force in the chain.

However the maximum bending moment developed in the longitudinal deck girder for the half-length load is seven times that of the full-length load (see table 4). This means that the deck and chain deflections for the half-length load are much greater. This model does not take into account the stiffening effect of the parapet and the longitudinal deck timbers so the real deflection is likely to be significantly less than in table 4. Barlow's uniform loading test caused the deck to sink by 7 inches (18cm) (Barlow and Ben, 2003) – approximately half the deflection calculated in SAP, so the maximum deck deflection is estimated to be 2m.

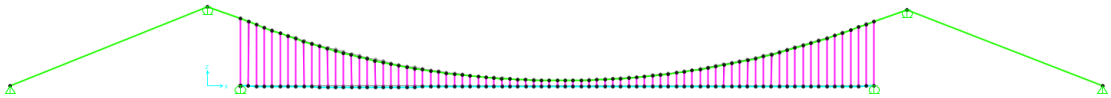

Figure 33. Deflection of the model with maximum live load all the way along the deck.

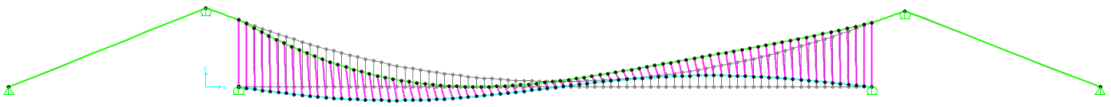

Figure 34. Deflection of the model with maximum live load on the left half of the deck.

To estimate the bending moment capacity, $M_{c,Rd}$ of the longitudinal beam, the calculation method from *EN 1993-1-1* was used. The beam has a Class 3 cross-section and an elastic section modulus, $W_{el} = 7.542662\times10^{6}mm^{3}$. It was assumed that $\gamma_{M0} = 1.0$.

$$M_{c,Rd} = M_{el,Rd} = W_{el,min}\frac{f_y}{\gamma_{M0}} = 7542662\times\frac{330}{1.0} = 2489kNm \quad (2)$$

Although the bending capacity calculated in equation 2 is higher than the maximum bending moment in the model (see table 4), wrought iron is more brittle than structural steel. It is likely that the longitudinal beam would fail before this moment was reached. Brunel's original design, without the stiffening effect of the parapet, would not have been strong enough to support the Barlow's design load. The addition of the stiffening parapet is key to the strength of the bridge.

5.3.2.2. Calculation of loads

The axial force in the chain was found by measuring the lengths of the force diagram in fig. 29., and has been plotted against the position along the chain in fig. 35. The minimum load occurs slightly to the left of the centre of the span, which correlates with the results of shape analysis, because the minimum load should be found in the lowest link.

To make the design of the chains more efficient, the cross sectional area of the chains is greater at the towers than in the centre. The area of one set of chains at the towers is 240 square inches (155,161mm^2) and the area in the centre of the span is 220 square inches (141,935mm^2) (Barlow and Ben, 2003). The critical load, N_{cr} has been calculated at both locations and for both LC1 and LC2.

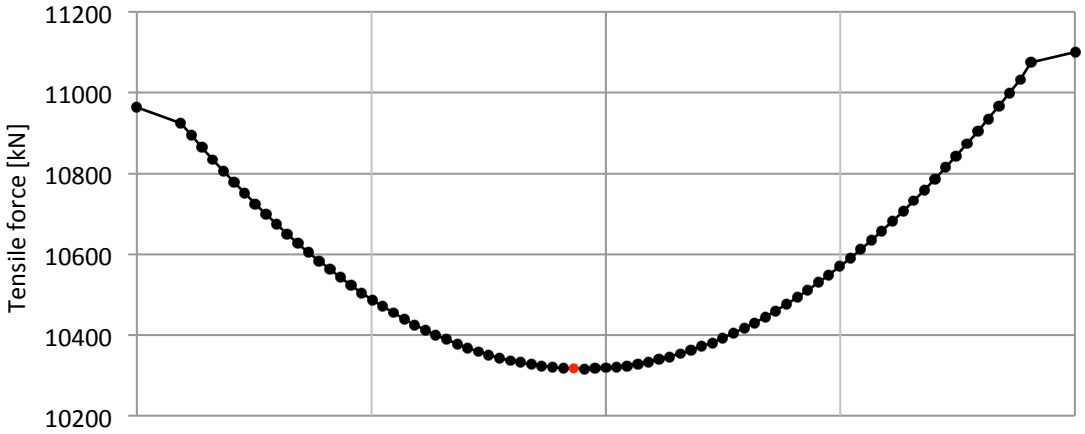

Figure 35. Distribution of axial loads throughout the as calculated from the CAD graphic statics. The maximum load at the Clifton tower is already known to be 11,100kN (calculated beforehand) and the load at the Leigh Woods tower is 10,964kN (calculated with graphic statics). The minimum load is 10,317kN and occurs two links to the left of the centre.

Table 5. Calculation of the critical load, N_{cr} and the factor of safety, F during LC1. The UTS is taken to be 330MPa (ASTM International, 1939) and the material strength coefficient, γ is 1.15.

Location	Centre of span	Tower
Cross-sectional area [mm^2]	141935	155161
Tensile load, T_{max} [kN]	10315	11100
Stress, σ [MPa]	72.7	71.5
UTS÷ γ [MPa]	287	287
Critical load, N_{cr} [kN]	40729	44525
Factor of safety, F	3.9	4.0

Table 6. Approximate calculation of the critical load, N_{cr} and the factor of safety F during LC2.

Location	Centre of span	Tower
Cross-sectional area [mm^2]	141935	155161
Tensile load, T_{max} [kN]	11560	12440

Stress, σ [MPa]	81.4	80.2
UTS÷ γ [MPa]	287	287
Critical load, N_{cr} [kN]	40729	44525
Factor of safety, F	3.5	3.6

The design factor of safety for LC1 could be seen as excessive, however it should be taken into account that eyebar chains are likely to fail at the connections. The values shown represent the strength of the eyebar itself, and not the strength of the connections between them. The Wheeling Bridge collapse was due to one broken connection (Gimsing, 1984), and Cullimore (1986) notes that the greatest signs of wear in the bridge are at the eyebar and hanger connection holes. These points act as stress concentrators and can cause the element to fail at a lower load expected. This is arguably one of the main reasons that chains have been replaced by cables in all suspension bridge designs since the 19th century. The use of many threads, means that they have a much higher level of redundancy – a cable can continue to function well even if a few of the threads have broken. It is likely that the actual maximum load of the chains is significantly lower than the values calculated, which goes some way to explaining the high values of F. Body (1976) writes that all the chains have been tested with twice the design load, so the lower bound for F is 2.

5.3.3. Other calculations

5.3.3.1. Cross-bracing

The cross-bracing under the deck provides stiffness against horizontal wind loading. Although Barlow and Ben (2003) notes that the deck can move 'up to 6" [15cm] in heavy wind', little was done to calculate its effects. The cross-bracing has not been analysed in this paper for the following reasons:

1. No documentation has been sourced to compare results of calculations.
2. It is unknown what effects the topography of the gorge would have on the wind, so calculations are likely to be inaccurate.
3. The action of wind loading on suspension bridges is related to the resonance and aerodynamic properties of the bridge, the calculation of which is outside the scope of the methods of analysis employed in this paper.

However wind loading remains an important factor in bridge engineering and in the case of the Clifton Suspension Bridge; for the first time in living memory in 2014 the bridge was closed to traffic during high winds. Therefore the analysis of wind loading on the bridge would be an interesting extension to this project.

3.3.3.2. Hangers

The highest axial load will occur in the second longest hangers, as the longest hangers are attached to the end of the suspended section and so have half the tributary area of the others (see fig. 14). Although the highest loads occur in these hangers, the difference is caused by the hangers' self-weight and is insignificant. Therefore all the hangers will have a similar value for F (see table 7).

Table 7. Calculation of the critical load, N_{cr} and the factor of safety F of the hanger.

	Estimated value
Cross-sectional area [mm^2]	1735
Tensile load, T_{max} [kN]	86.6
Stress, σ_{max} [MPa]	49.9
UTS÷ γ [MPa]	287
Critical load, N_{cr} [kN]	497

Factor of safety, F	5.8

The calculated critical load is almost 6 times greater than T_{max}, which suggests that the hangers are inefficiently designed. However the calculation does not take into account the connections at either end. Like in the chains, these are likely to be the cause of failure. Several hangers have broken, the most recently in 2009 ("Suspension bridge closed by fault", 2009) and Cullimore (1986) notes that many show signs of wear at the connections. It is likely that the hangers will fail at the bolt-holes or welds, so in this case N_{cr} is not representative of the failure load.

5.3.3.3. Towers

According to plans available on the website of the Clifton Suspension Bridge ("Your Bridge Projects | The Clifton Suspension Bridge"), the masonry towers are faced with local Pennant sandstone and the cavities are filled with loose rubble. Richards says that the towers themselves were not subject to much formal analysis, but if it is assumed that rubble is not load-bearing and the load bearing wall is 0.3m thick, the maximum stress developed in the base is insignificant (see table 8), considering sandstone typically has a high compressive strength – Pennant stone has a compressive capacity of 168MPa (Bell, 2013).

Table 8. Calculation of the maximum stress developed in the tower. The load at the base of the tower is the sum of the load at the tower saddle and the self-weight of the tower. The load-bearing part of the tower is assumed to have a density of 2.5kg/m3.

Location	Tower saddle	Base of tower
Total load [kN]	19,180	27,680
Area [m^2]	10.3	16.3
Stress, σ [MPa]	1.2	2.7

6. Comparison of analytical methods

As mentioned earlier, graphic statics is a limited method of analysis in comparison with modern numerical methods. Numerical methods are more precise, faster and are able to compute much more than graphic statics. The precision and accuracy of graphic statics were primarily explored in this project, however other qualitative observations can be made too.

The graphic statics method was significantly slower than the numerical method. Although the computer model required some time to set up, it was still completed quicker than the manual drawings, which in most cases took 2-3 hours to prepare, complete and take results. Once a computer model was set up, the calculation could be repeated quickly for different load combination, while the graphic statics method requires that you start from scratch with each load combination. The faster method is preferable in almost all cases in engineering. It should be noted that the graphic statics for the transversal girder could be carried out within 20 minutes using a CAD program, however this is still slower than the numerical method.

The computational limitations of the graphical method were made obvious during this project as several parts of the bridge could not be analysed with it at all. The longitudinal girder is a single object and primarily acts in bending. As graphic statics can only be use to find the axial load on an object, it was useless in this case.

The precision of the graphic statics was determined by the scale of the force diagram drawn. The drawings were done on A0 paper at scales of 1cm:1kN or 1cm:2kN for the transversal girders. This allowed for a theoretical precision of 0.05kN an 0.1kN respectively, however the mean accuracy was typically 0.5 to 1kN. The theoretical precision could be increased by using a larger scale, but it was noticed that in some cases the longest lines had the lowest accuracy. It is likely that the larger the diagram, the more difficult it is to draw, so the accuracy is reduced. Drawing at these scales was difficult because the 140cm rule was unwieldy and the A0 sheets were too large to use comfortably. I would argue that there is a limited scale at which useful drawing is possible, as percentage error increases with scale. Although the method is inaccurate when done by hand, they would be sufficiently accurate and precise for many civil engineering applications.

Based on these observations, it is obvious that graphic statics is not a replacement for numerical methods. However it does have value as a visual aid. Mathematics is an integral part of engineering, however it can cause problems when the method is not fully understood or the results are incorrectly interpreted. Graphic statics could be useful in teaching or presentations, where the specific results are not as important as understanding the behaviour of the structure. A combination of the form and force diagrams is a visual way to present the information, which would be useful for those who do not have an understanding of the mathematics or do not know the structure.

7. Critical evaluation of the bridge

7.1. The modern structure

According to David Billington's *The tower and the bridge* (1985), a work of structural engineering is a work of structural art if it fulfils the three criteria: economy, efficiency and elegance. Economy is a measure of the cost of the structure – during both construction and operation – in comparison to it's social worth. Structures that meet this ideal have good value for money. Efficiency is a quantitative evaluation of the design – how well the structure is suited to its purpose – and elegance is the evaluation from a qualitative point of view.

It can be argued that the economy of the Clifton Suspension Bridge has changed during its 200 year history. According to Body (1976), when Vick died in the 18th century, the area around the bridge was largely uninhabited. Clifton only became a popular suburb of Bristol in the 19th century and Leigh Woods remains a small village. It is not clear why Vick wanted a bridge built in that location, as there was seemingly little need for it – a bridge there would be of little use to anyone. During the construction, the cost of the bridge increased enormously; the final cost – approximately £75,000 – was more than double Brunel's estimate of 1830 (Body, 1976). The venture is arguably wasteful and uneconomical when the high cost and the low practicality are considered.

However the modern situation of the bridge is quite different. Although access is limited and the capacity of the bridge is small in comparison to other bridges across the Avon, it is used by more than 10,000 vehicles a day ("Suspension bridge toll may double to £1," 2010) and provides an alternative route over the river to those in the centre of Bristol and in Avonmouth. It is of great historical and structural interest and is a popular tourist attraction. The toll leveed on motorised vehicles provides money for maintenance and operation. Instead of becoming less useful and more expensive to run, the bridge has become very economical.

The efficiency of the bridge is more easily analysed. Suspension bridges are one of the most efficient bridge designs; this explains their use in the largest spans in the world. The cables and hangers act solely in tension and the towers in compression. This means bending moments and shear forces in the structure are very low and the bridge can be built using minimal material. This project has shown that the design of the cable and the deck girders is efficient – using the least material possible while retaining an adequate factor of safety – especially considering the analytical methods available at the time. Other factors, such as the stiffening effect of the deck timbers and integrated parapet mean that the size of the girders can be reduced.

Finally the elegance of the Clifton bridge is discussed. Although not Brunel's first choice, the design is lauded by many and it is clear that he took great care over the appearance of the bridge. The slope of the bridge was designed to make the bridge look horizontal when viewed from upstream. Painting the metalwork white makes the structure less obtrusive when viewed from along the river and the simple tower design, using local sandstone, is in keeping with the architectural style of the buildings in Bristol. The inscription on the Leigh Woods tower; 'SUSPENSA VIX VIA FIT' (the road becomes barely suspended) is a tribute to the amazement of early visitors to the bridge and illustrates the effectiveness of the design – impressive but not dominating, so that the Avon Gorge remains the principal subject of interest.

From this evaluation, the Clifton Suspension Bridge is found to be of great social and historical value, well designed and with pleasing aesthetic qualities; fulfilling Billington's criteria to be considered an example of structural art.

7.2. Other submissions from the design competition

7.2.1. 'Giant's Hole' design – Brunel

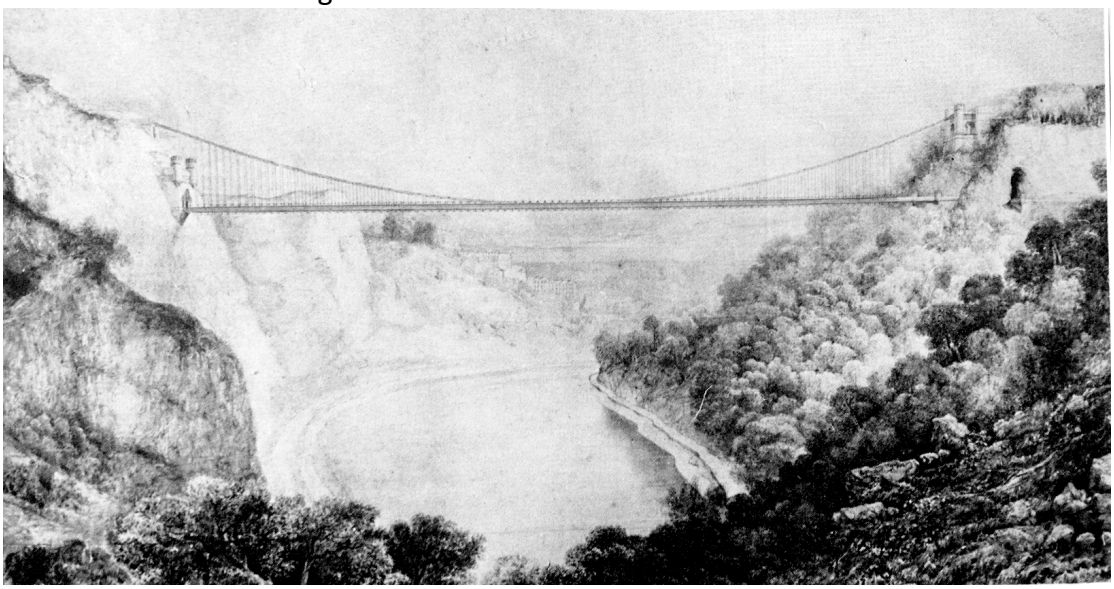

Figure 36. Brunel's 'Giant's Hole' design. From *Clifton Suspension Bridge*, Geoffrey Body, 1976..

Brunel's favourite design for the bridge over the Avon Gorge was submitted for the first competition. The bridge would be accessible via an underground passage that passed into a cave in rock face. The suspension chains would be anchored in sides of the gorge itself, removing the need for piers, towers and land chains. It is easy to see why it was his favourite, being far simpler and less obtrusive than the other designs (McIlwain, 1996). The primary criticism of the design was its ambitious span, which would have been several hundred feet longer than any other bridge at that time. When evaluated in terms of Billington's structural art criteria, the design is extremely good. By anchoring the suspension chains in the cliff-faces, the structure is made very efficient and economical. The construction of the piers and towers in the Clifton Suspension Bridge accounted for the majority of the cost of construction (Body, 1976), so this design would constitute a great improvement in the price of the work. However the viability of such a span was a principle concern to the judging panel, so it is unsurprising that the design was not awarded the prize.

7.2.2. Gothic Revival – Telford

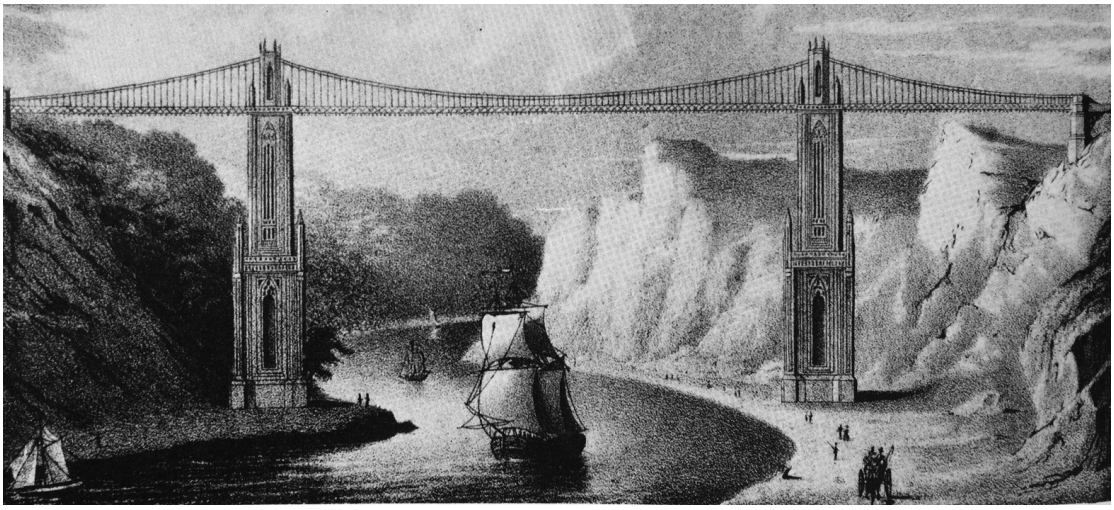

Figure 37. Telford's gothic design. From *Clifton Suspension Bridge*, Geoffrey Body, 1976.

Telford said that the width of the gorge was too great to be covered by a single span, so suggested a three-span design with a gothic tower on either side of the river (Body, 1976). The twin-tower design (see fig. 37), won the first competition but attracted great public criticism for its appearance (McIlwain, 1996). The design would have also been particularly expensive. The savings made by building a suspension bridge instead of a stone bridge would have been all but annulled by the cost of building two 80m towers. Although a suspension bridge is a particularly efficient bridge design, the sheer size of the towers in this case make it far too expensive to comply with Billington's economy criterion.

7.2.3. Stone beam – Burge

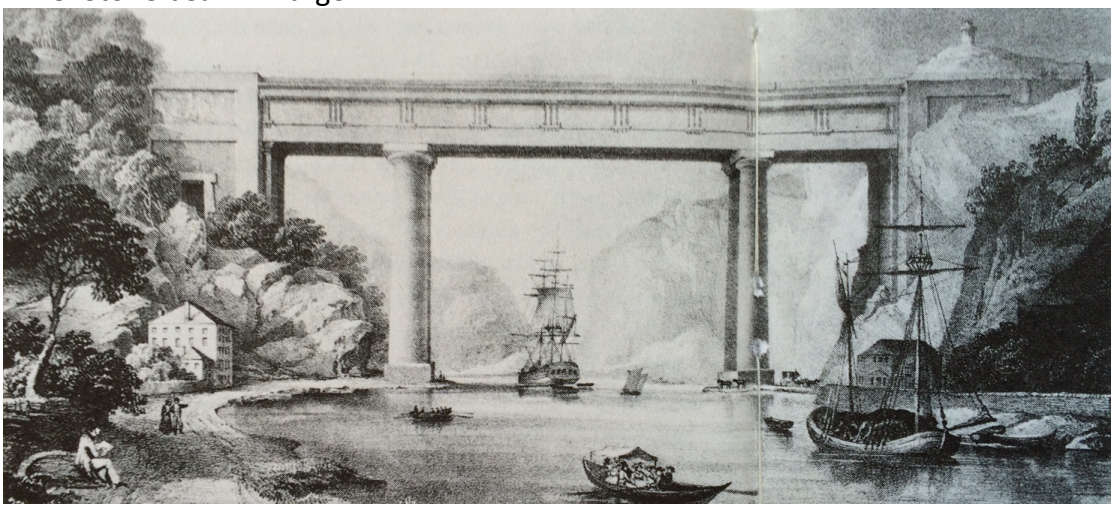

Figure 38. Burge's stone beam bridge design. From *Clifton Suspension Bridge*, Geoffrey Body, 1976.

This stone beam bridge designed by William Burge was immediately rejected on a basis of cost (Body, 1976), however it is interesting to examine it in relation to Billington's efficiency criterion. Unlike stone arch bridges, where the arch acts only in compression, a huge bending moment would develop in the deck just due to the weight of the stone itself. This would cause a tensile load in the bottom of the deck. Stone has good compressive strength but a poor tensile capacity, so this extreme design would be impossible to construct as the bridge would collapse under its own weight. It might be possible to construct using pre-stressed and reinforced concrete, but stone does not have the tensile strength to be used here. This is a good example of how the choice of material affects the efficiency criterion – to be efficient as structure must make use of suitable materials.

7.2.4. Combined arch-suspension bridge – Hill

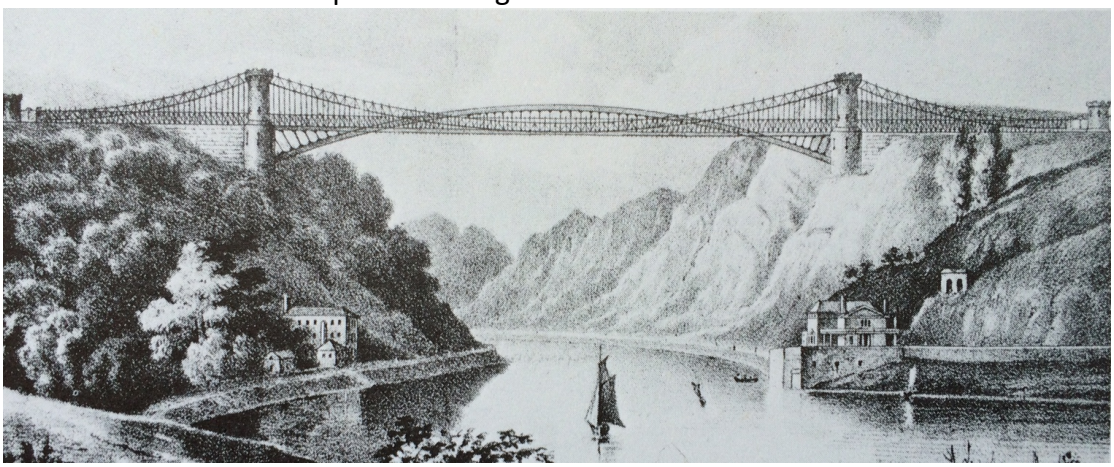

Figure 39. Hill's iron arch-suspension bridge. From *Clifton Suspension Bridge*, Geoffrey Body, 1976.

William Hill submitted this rather unorthodox design, where the deck is not only suspended by suspension chains but also an iron arch and a stiffening truss. Like many other designs it was rejected owing to the estimated cost (Body, 1976). It is another example of inefficient design, but because of the structure itself, rather than the material. The combination of three different elements – the truss, suspension cables and arch – would have made an incredibly stiff bridge, more robust than it needed to be. This unnecessary design would just have contributed to the already large costs of the bridge.

8. Conclusion

The development of structural analysis methods over the last 200 years has greatly affected the evolution of bridge design. The Brooklyn Bridge is an example of extreme over-engineering to compensate for a lack of certainty, while the Severn Bridge has an economical and efficient design that could only be achieved with the latest mathematical analysis. There is an assumption in engineering today that if the latest methods of analysis have not been used, the result is neither reliable nor engineering. The aim of this paper was to explore to what extent non-numerical methods of analysis are useful, and to use a qualitative method to compare different bridge designs.

The Clifton Suspension Bridge was analysed using a modern numerical method and a graphical method more representative of the analytical capabilities of the 19th century. Although the graphical method was less precise, more time consuming and less powerful than the numerical method, it was still sufficiently accurate to model the forces and ideal shapes of some key elements of the bridge. This comparison of the two methods permits a greater understanding of early suspension bridge designs and an gives an insight into the role of civil engineers in the 19th century.

The difference between Brunel's original design and the one constructed by Brunel and Hawkshaw was discussed and supports the theory that it is as much their bridge as his; it is was suggested that Brunel's design would not have been strong enough to last until today.

Finally, various submissions from the design competition were evaluated using Billington's three criteria for structural art, in a similar way to which the competition might have been judged. It provided an integral and complete approach to qualitative analysis; an evaluation that takes into account not just the mechanical performance of the structure, but to what extent it fulfils its role as a public facility.

9. References

ASTM International, 1939. English: *ASTM A207: Withdrawn 1972. Specification for Rolled Wrought Iron Shapes and Bars*

Baker, W.F., Beghini, L.L., Mazurek, A., Carrion, J., Beghini, A., 2013. *Maxwell's reciprocal diagrams and discrete Michell frames.* Struct. Multidiscip. Optim. 48, 267–277.

Barlow, W.H., Ben, B., 2003. *Description of the Clifton Suspension Bridge, UK.* Proc. Inst. Civ. Eng. - Bridge Eng. 156, 5–10.

Bell, F.G., 2013. *Methods of Treatment of Unstable Ground.* Elsevier.

Body, G., 1976. *Clifton Suspension Bridge, 1st ed.* Moonraker Press, Bath.

British Standards Institution, 2002. English: *EN 1991-1-1: Eurocode 1: Actions on structures - Part 1-1: General actions - Densities, self-weight, imposed loads for buildings*

British Standards Institution, 2005. English: *EN 1993-1-1: Eurocode 3: Design of steel structures - Part 1-1: General rules and rules for buildings*

Buonopane, S.G., Billington, D.P., 1993. *Theory and History of Suspension Bridge Design from 1823 to 1940.* J. Struct. Eng. 119, 954–977.

Canaan, 2009. Español: *Maqueta polifunicular, Antoni Gaudí, Museo de la Sagrada Familia.*

Cullimore, M.S., 1986. *The Clifton Suspension Bridge: preservation for utilisation.* IABSE Proc. 10, 13.

D, J., 2007. *Clifton Suspension Bridge chains, Bristol.*

Drewry, C.S., 1832. *A Memoir of Suspension Bridges: Comprising the History of Their Origin and Progress, and of Their Application to Civil and Military Purposes, with Descriptions of Some of the Most Important Bridges; Viz. Menai, Berwick, Newhaven, Geneva, Etc. Also an Account of the Experiments of the Strength of Iron Wires and Iron Bars, and Rules and Tables for Facilitating Computations Relating to Suspension Bridges.* Longmans, Rees, Orme, Brown, Green & Longman, London.

Edwards, M., 2007. English: *The Severn Bridge spans the River Severn between South Gloucestershire, England, and Monmouthshire in South Wales,.*

Gimsing, N.J., 1984. *Cable supported bridges: concept and design.* J. Wiley, Chichester [Sussex]; New York.

Gothick, 2009. *Clifton Suspension Bridge, Bristol, England.*

Grattesat, G., 1978. *Conception des Ponts.* Edition Eyrolles, Paris.

High winds force closure of Bristol's Clifton Suspension Bridge, 2014. . BBC News.

McIlwain, J., 1996. *Clifton Suspension Bridge.* Pitkin Unichrome Ltd.

Ministerio de Fomento, 2011. Spanish: *IAP-11: Instrucción sobre las acciones a considerar en el proyecto de puentes de carretera*

Miyata, T., Yamada, H., Katsuchi, H., Kitagawa, M., 2002. *Full-scale measurement of Akashi–Kaikyo Bridge during typhoon.* J. Wind Eng. Ind. Aerodyn., Fifth Asia-Pacific Conference on Wind Engineering 90, 1517–1527.

Poleni, G., 1748. *Memorie istoriche della gran cupola del tempio Vaticano, e de' danni di essa e de' ristoramenti loro, divise in libri cinque. Nella Stamperia del Seminario.*

Richards, D., 2010. *A critical analysis of the Clifton Suspension Bridge.* Proc. Bridge Eng. 2 Conf. 2010.

Shackelford, J.F., Han, Y.-H., Kim, S., Kwon, S.-H., 2016. *CRC Materials Science and Engineering Handbook, Fourth Edition.* CRC Press.

"Suspension bridge shut for events", 2005. . BBC News.

"Suspension bridge toll may double to £1", 2010. . Bristol Evening Post.

"Suspension bridge closed by fault", 2009. . BBC News.

User:Postdlf, 2005. English: *The Brooklyn Bridge, seen from Manhattan, New York City.*

Van Mele, T., Lachauer, L., Rippmann, M., Block, P., 2012. *Geometry-based understanding of structures.* J. Int. Assoc. Shell Spacial Struct.

WPPilot, 2015. English: *This is the Golden Gate Bridge on Dec 15 2015 by D Ramey Logan from just north of Alcatraz Island.*

"Your Bridge Projects | The Clifton Suspension Bridge". Cliftonbridge.org.uk. N.p., 2016. Web. 2 June 2016.

10. Appendices

The appendices are found in volume 2. Appendices A—E are the hand-drawn force diagrams used for graphical analysis. Those which span more than one page have pages numbered from left to right. Appendices F–J are the force diagrams made with CAD. Appendices K—M are spreadsheets.

Hand-drawn force diagrams:
Appendix A – Analysis of transversal girder under LC1. (Two pages).
Appendix B – Analysis of transversal girder under LC2. (Two pages).
Appendix C – Analysis of transversal girder under LC3.
Appendix D – Analysis of transversal girder under LC4.
Appendix E – Analysis of suspension chain.

CAD force diagrams:
Appendix F – Analysis of transversal girder under LC1.
Appendix G – Analysis of transversal girder under LC2.
Appendix H – Analysis of transversal girder under LC3.
Appendix I – Analysis of transversal girder under LC4.
Appendix J – Analysis of suspension chain.

Spreadsheets:
Appendix K – Applied loads to transversal girder.
Appendix L – Results of transversal girder numerical analysis.
Appendix M – Analysis of chain shapes.